

# Reduced-Space Iteratively Reweighted Second-Order Methods for Nonconvex Sparse Regularization

Hao Wang<sup>1</sup>, Xiangyu Yang<sup>2,3</sup>, Yichen Zhu<sup>1\*</sup>

<sup>1</sup>School of Information Science and Technology, ShanghaiTech  
University, Shanghai, 201210, China.

<sup>2</sup>School of Mathematics and Statistics, Henan University, Kaifeng,  
475000, China.

<sup>3</sup>Center for Applied Mathematics of Henan Province, Henan University,  
Zhengzhou, 450046, China.

\*Corresponding author(s). E-mail(s): [zhuych2022@shanghaitech.edu.cn](mailto:zhuych2022@shanghaitech.edu.cn);  
Contributing authors: [haw309@gmail.com](mailto:haw309@gmail.com); [yangxy@henu.edu.cn](mailto:yangxy@henu.edu.cn);

## Abstract

This paper explores a specific type of nonconvex sparse regularization problems, namely those involving  $\ell_p$ -norm regularization, in conjunction with a twice continuously differentiable loss function. We propose a novel second-order algorithm designed to effectively address this class of challenging nonconvex and nonsmooth problems, showcasing several innovative features: (i) The use of an alternating strategy to solve a reweighted  $\ell_1$  regularized subproblem and the subspace approximate Newton step. (ii) The reweighted  $\ell_1$  regularized subproblem relies on a convex approximation to the nonconvex regularization term, enabling a closed-form solution characterized by the soft-thresholding operator. This feature allows our method to be applied to various nonconvex regularization problems. (iii) Our algorithm ensures that the iterates maintain their sign values and that nonzero components are kept away from 0 for a sufficient number of iterations, eventually transitioning to a perturbed Newton method. (iv) We provide theoretical guarantees of global convergence, local superlinear convergence in the presence of the Kurdyka-Łojasiewicz (KL) property, and local quadratic convergence when employing the exact Newton step. We also showcase the effectiveness of our approach through experiments on a diverse set of model prediction problems.

**Keywords:** nonconvex regularized optimization, subspace minimization, regularized Newton method, iteratively reweighted method

# 1 Introduction

In this paper, we consider optimization problems of the form

$$\min_{\mathbf{x} \in \mathbb{R}^n} F(\mathbf{x}) := f(\mathbf{x}) + \lambda h(\mathbf{x}), \quad (1)$$

where  $f : \mathbb{R}^n \rightarrow \mathbb{R}$  is proper and twice continuously differentiable but possibly non-convex,  $\lambda > 0$  refers to the regularization parameter, and the regularization function  $h : \mathbb{R}^n \rightarrow [0, +\infty)$  is a sum of composite functions as follows

$$h(\mathbf{x}) := \sum_{i=1}^n (r \circ |\cdot|)(\mathbf{x}), \quad \forall \mathbf{x} \in \mathbb{R}^n. \quad (2)$$

The function  $f$  and  $r$  satisfy the following assumptions:

**Assumption 1.(i)** *Throughout  $f$  is level-bounded [1, Definition 1.8].*

*(ii)  $r : [0, +\infty) \rightarrow [0, +\infty)$  is smooth on  $(0, +\infty)$  with  $r'(t) > 0$  and  $r''(t) \leq 0$  for  $t \in (0, +\infty)$ , and is subdifferentiable at 0. Moreover,  $r$  satisfies  $r(0) = 0$ ,  $r'(t)$  is convex,  $\lim_{t \rightarrow +\infty} r(t) = +\infty$  and  $\lim_{t \rightarrow +\infty} \frac{r'(t)}{t} = 0$  over  $t \in (0, +\infty)$ .*

The assumption 1 implies that  $\lim_{\mathbf{x} \in \mathbb{R}^n : \|\mathbf{x}\| \rightarrow \infty} F(\mathbf{x}) = +\infty$  and further implies  $\min_{\mathbf{x} \in \mathbb{R}^n} F(\mathbf{x}) = \underline{F} > -\infty$  and  $\{\mathbf{x} \mid \operatorname{argmin}_{\mathbf{x} \in \mathbb{R}^n} F(\mathbf{x})\} \neq \emptyset$  with respect to (P). The assumption 1(ii) in the function  $r$  is sufficiently general, allowing (2) to cover several important instances of (1). Specifically, the function  $h$  can represent various nonconvex regularization functions that have been proposed as effective surrogates for the  $\ell_0$  norm, efficiently reducing the relaxation gap. Typical examples include the  $\ell_p$  norm with  $p \in (0, 1)$  [2], Smoothly Clipped Absolute Deviation [3], Minimax Concave Penalty [4], and Capped  $\ell_1$  [5], to name just a few. Extensive computational research has shown that nonconvex regularization functions can effectively avoid solutions from biased solution spaces, unlike convex counterparts such as the  $\ell_1$ -norm. Moreover, [6] theoretically demonstrated that minimizing nonconvex regularizers requires significantly fewer measurements than traditional  $\ell_1$ -norm minimization. These advancements highlight the prevalence of composite optimization problems of the form (1) in applications such as sparse learning, model compression, compressive sensing, and signal/image processing (see, e.g., [7–10]).

The nonconvex  $\ell_p$  norm, with  $p \in (0, 1)$ , is widely recognized as an efficient and effective regularizer for achieving desired sparse solutions, as supported by extensive research [7–11]. In addition, the  $\ell_p$  norm is a particular case of (2) where  $\lim_{t \rightarrow 0+} (|t|_p^p)' = +\infty$ , which in principle makes it more challenging to solve compared to other nonconvex regularizers. Given these considerations, this paper mainly focuses on the  $p$ th power of  $\ell_p$  norm regularization optimization problem:

$$\min_{\mathbf{x} \in \mathbb{R}^n} F(\mathbf{x}) := f(\mathbf{x}) + \lambda \|\mathbf{x}\|_p^p. \quad (\mathcal{P})$$

In the past decade, composite optimization problems of this form have been extensively studied, with two main approaches emerging: approximation methods and proximal mapping methods.

Various approximation methods have been developed to handle the nonconvexity and nonsmoothness of the  $\ell_p$ -term, as detailed in works by Lu [12], Wang et al. [13–15], Lai [16], Chen [17], and others [18–21].

As an example, the well-known iteratively reweighted  $\ell_\alpha$  approach approximates the  $\ell_p$ -term by  $|x_i|^p \approx p(|x_i^k|^\alpha + \epsilon_i)^{\frac{p}{\alpha}-1}|x_i|^\alpha$  where  $\mathbf{x}^k$  is the current iterate. This approach constructs a convex approximation by employing weights derived from the linearization of the  $\ell_p$  norm at the current iterate, a strategy extensively considered in many first-order methods [13–16]. Wang et al. [13] proposed an iteratively reweighted  $\ell_1$  method with soft-thresholding updates, and significant advancements have been made by incorporating extrapolation techniques into these methods [15, 22], establishing convergence under the Kurdyka-Łojasiewicz (KL) property. In these methods, perturbation  $\epsilon$  is crucial for algorithm design and convergence. Wang et al. [13] developed a dynamic update strategy that drives perturbations toward zero only for nonzero components. Second-order methods have also been developed within this framework. Chen [17] introduced a second-order method utilizing a smoothing trust region Newton approach for Problem 1, approximating the regularizer with a twice continuously differentiable function (i.e. weighted  $\ell_2$ -norm) and demonstrating global convergence to a local minimizer.

For the specific case of  $p = \frac{1}{2}$  and  $\frac{2}{3}$ , the proximal gradient method is commonly used, with Xu [20] providing a closed-form proximal mapping for these values. Although generic  $\ell_p$  proximal mapping methods exist [23], they are slower and less practical for large-scale problems. Several first-order methods leveraging these developments have been introduced in recent works [11, 24]. Second-order methods have been widely studied for general nonconvex and nonsmooth composite problems within the proximal mapping framework. A class of proximal Newton methods, inspired by proximal mapping, has emerged to solve regularized proximal Newton problems globally under the assumption of a convex regularizer, achieving superlinear convergence under various conditions, such as metric  $q$ -subregularity [25], the Luo-Tseng error bound [26], or the KL property [27].

To combine the strengths of proximal gradient and Newton methods, hybrid approaches have been proposed. Considering the sparsity-driven Problem 1, it involves nonsmooth regularization functions that typically have a smooth substructure on active manifolds. For example, in  $(\mathcal{P})$ , the function is smooth around any nonzero point. While  $\mathbf{x} = 0$  is a stationary point of  $F$ , it is not optimal in terms of objective value, making the identification of the correct active manifold crucial. The proximal gradient method and its variants are effective in reaching the optimal submanifold [28, 29]. The iteratively reweighted method shares similar properties with the proximal gradient method, leading us to design an automatic active manifold identification process using this approach. After identifying the active manifold, transitioning to a Newton method is logical, as it offers superlinear convergence on the smooth manifold. Hybrid methods integrating proximal gradient with Newton methods have been explored for nonconvex, nonsmooth problems [30–32], but few second-order methods specifically address  $(\mathcal{P})$ . Recently, Wu et al. [33] and Zhou et al. [34] introduced

proximal-based algorithms that combine proximal gradient with subspace regularized Newton or semismooth Newton methods, achieving superlinear or quadratic convergence. A detailed comparison of convergence results is shown in Table 1.

**Table 1:** Related algorithms for Problem 1. Notice that the subsequent rows consider broader problems than the previous rows. (a)  $f$  Lipschitz differentiable on bounded set. (b)  $f$  strongly smooth. (c)  $f$  Lipschitz twice differentiable on support. (d) Curve ratio condition. (e) KL property. (f) Positive definite local minimizer. (g)  $\nabla f$  strongly semismooth on bounded set. (h)  $f$  smooth and convex. (g) Nonsingular local minimizer.

Problems.	Algorithms	Global convergence	Local convergence
$h(x) = \ x\ _p^p, p \in \{\frac{1}{2}, \frac{2}{3}\}$	HpgSRN[33] PCSNP[34]	(c)(d)(e) (a)	superlinear, (e) quadratic, (f)(g)
$h(x) = \ x\ _p^p, p \in (0, 1)$	IR $\ell_\alpha$ [12] EPIR $\ell_1$ [15]	(b) (a),(e)	- linear/superlinear, (e)
Generic $h(x)$	AIR [35] STRN [17] SOIR $\ell_1$ (Ours)	(h) (c) (a)	linear, (h) - superlinear, (e) quadratic, (c)(g)

In this paper, we design and analyze SOIR $\ell_1$ , a second-order method for the  $\ell_p$ -norm regularization problem (( $\mathcal{P}$ )), which are also applicable to general nonconvex and nonsmooth regularization problems (Problem 1). Our method is a hybrid approach that alternates between solving an iteratively reweighted  $\ell_1$  subproblem and a subspace Newton subproblem. This hybrid framework integrates the subspace Newton method with a subspace iterative soft-thresholding technique, employing an approximate solution for the Newton subproblem to enhance speed. Unlike proximal-type methods, each iteration of our method approximates the  $\ell_p$ -norm with a weighted  $\ell_1$ -norm and locally accelerates the process using the Newton subproblem, enabling our method to solve for generic  $p$  ( $0 < p < 1$ ).

The adaptability of the Newton subproblem allows our method to incorporate various types of quadratic programming (QP) subproblems, achieving different convergence outcomes based on the subsolver used. The proposed method achieves global convergence under the conditions of Lipschitz continuity of  $f$  and boundedness of the Hessian. Locally, we establish the convergence rate under the Kurdyka-Łojasiewicz property of  $F$  with different exponents, achieving superlinear convergence with an exponent greater than  $1/2$ . By employing a strategic perturbation setting, we attain local quadratic convergence under the local Hessian Lipschitz continuity of  $F$  on the support. When extending our method to tackle the generic problems (Problem 1), the same convergence results are maintained.

Numerical experiments show that SOIR $\ell_1$  outperforms existing methods, such as the hybrid method combining proximal gradient and regularized Newton methods [33], the proximal semismooth Newton pursuit method [34], and the extrapolated iteratively reweighted  $\ell_1$  method [15], offering superior time efficiency while maintaining

comparable solution quality. Additional experiments validate the effectiveness of our algorithm across different regularization problems.

Our method offers several distinct advantages over existing second-order methods. Unlike the smoothing trust region Newton method [17], which requires a twice continuously differentiable approximation for regularization terms, our approach uses a nonsmooth local model that retains weighted  $\ell_1$  regularization and optimizes within a subspace, potentially leading to more efficient search directions. Additionally, our method dynamically identifies and exploits the active manifold during optimization, a feature absent in the smoothing trust region method. Compared to proximal-based methods like HpgSRN [33] and PCSNP [34], our method has the following differences and advantages: (i) We use an iteratively reweighted  $\ell_1$  model as a subproblem, with perturbations to smooth out local suboptimal points, leading to better solutions. (ii) Our IST updates solve the local model, providing a practical method for generic  $\ell_p$ -norm regularization, applicable to a broader range of  $p$  values. (see Section 5.3 for numerical comparison). (iii) Our method applies subspace IST separately to zero and nonzero components, unlike existing methods that apply the proximal gradient to all components. Our approach has a clearer process for manifold identification: IST on zero components explores a larger manifold and IST on nonzero components reduces the manifold. With the exploration process partially controlled by perturbations, it allows us to accelerate or refine the process and enter the second-order phase appropriately. In the second-order phase, a subspace Newton direction with projection further enhances local support stability.

## 1.1 Organization

The structure of this paper is as follows: In Section 2, we introduce the proposed algorithm in detail. Section 3 outlines both the global and local convergence properties of the algorithm. Section 4 explores possible extensions and variants of the algorithm. Finally, Section 5 presents the results of numerical experiments.

## 1.2 Notation and stationarity conditions

Throughout let  $\mathbb{R}^n$  denote the  $n$ -dimensional Euclidean space, equipped with the standard inner product  $\langle \cdot, \cdot \rangle$  and its induced norm  $\|\cdot\|$ .  $\mathbb{R}_+^n$  and  $\mathbb{R}_{++}^n$  are the set of nonnegative real vectors and strictly positive real vectors, respectively. For any  $\mathbf{x}, \mathbf{y} \in \mathbb{R}^n$ , we use  $x_i$  to denote its  $i$ th component. Let  $\mathbf{x} \circ \mathbf{y}$  denote the component-wise product of  $\mathbf{x}$  and  $\mathbf{y}$ , i.e.,  $[\mathbf{x} \circ \mathbf{y}]_i = x_i y_i$ ,  $\forall i \in [n]$ , and we use  $\mathbf{x} \leq \mathbf{y}$  to denote  $x_i \leq y_i$ ,  $\forall i \in [n]$ . Define the index sets of nonzeros and zeros of  $\mathbf{x}$  as  $\mathcal{I}(\mathbf{x}) = \{i \mid x_i \neq 0\}$  and  $\mathcal{I}_0(\mathbf{x}) = \{i \mid x_i = 0\}$ , respectively. The support  $\mathcal{I}(\mathbf{x})$  can be further divided into  $\mathcal{I}(\mathbf{x}) = \mathcal{I}_+(\mathbf{x}) \cup \mathcal{I}_-(\mathbf{x})$ , where  $\mathcal{I}_+(\mathbf{x}) = \{i \mid x_i > 0\}$  and  $\mathcal{I}_-(\mathbf{x}) = \{i \mid x_i < 0\}$ . Let  $|\mathcal{S}|$  denote the cardinality of a nonempty set  $\mathcal{S}$ .  $[n]$  denotes the index set  $\{1, 2, 3, \dots, n\}$ . For  $\emptyset \neq \mathcal{S} \subseteq [n]$ ,  $\mathbf{x}_{\mathcal{S}} \in \mathbb{R}^{|\mathcal{S}|}$  is a subvector by restricting  $\mathbf{x}$  to the entries in  $\mathcal{S}$ . Let  $\|\mathbf{x}\|_p := (\sum_{i=1}^n |x_i|^p)^{\frac{1}{p}}$  denote the  $\ell_p$  norm of  $\mathbf{x}$  (it is a norm if  $p \geq 1$  and a quasi-norm if  $0 < p < 1$ ), and  $\|\mathbf{x}\|$  represents the  $\ell_2$  norm of  $\mathbf{x}$  unless specified otherwise.

Consider the function  $F : \mathbb{R}^n \rightarrow \mathbb{R}$ . For any  $\mathbf{x}_{\mathcal{S}} \neq \mathbf{0}$ , the partial gradient of  $F$  over  $\mathbf{x}_{\mathcal{S}}$  is denoted as  $\nabla_{\mathcal{S}} F(\mathbf{x})$ , that is,  $\nabla_{\mathcal{S}} F(\mathbf{x}) = \partial F / \partial \mathbf{x}_{\mathcal{S}} \in \mathbb{R}^{|\mathcal{S}|}$  with a slight abuse

of notation. We do not suggest  $\nabla_i F(\mathbf{x}) = [\nabla F(\mathbf{x})]_i$  for  $i \in [n]$  since  $F$  may not be differentiable at  $\mathbf{x}$ . Denote  $\nabla_{\mathcal{S}S} F(\mathbf{x})$  as the sub-Hessian of  $F$  with respect to  $\mathcal{S}$  if  $\nabla F$  is (partially) smooth on  $\mathbf{x}_{\mathcal{S}}$ .

For any  $\mathbf{x} \in \mathbb{R}^n$ , the signum function of  $\mathbf{x}$   $\text{sign}(\mathbf{x})$  is defined in an element-wise way, i.e.,  $\text{sgn}(x_i) = 1$  if  $x_i > 0$ ,  $\text{sgn}(x_i) = -1$  if  $x_i < 0$  and  $\text{sgn}(x_i) = 0$  if  $x_i = 0$ . Given  $\mathbf{v} \in \mathbb{R}^n$  and  $\boldsymbol{\omega} \in \mathbb{R}_{++}^n$ , the weighted soft-thresholding operator is defined as

$$[\mathbb{S}_{\boldsymbol{\omega}}(\mathbf{v})]_i := \text{sgn}(v_i) \max(|v_i| - \omega_i, 0).$$

$\mathbb{P}(\mathbf{y}; \mathbf{x})$  is defined to project a given vector  $\mathbf{y} \in \mathbb{R}^n$  onto the quadrant containing  $\mathbf{x} \in \mathbb{R}^n$ , i.e.,

$$[\mathbb{P}(\mathbf{y}; \mathbf{x})]_i := \text{sign}(x_i) \max\{0, \text{sign}(x_i)y_i\}. \quad (3)$$

For any symmetric matrix  $\mathbf{A} \in \mathbb{R}^{n \times n}$ ,  $\mathbf{A} \succ \mathbf{0}$  indicates  $\mathbf{A}$  is positive definite. For  $\emptyset \neq \mathcal{I} \subseteq [n]$ , define  $\mathbf{A}_{\mathcal{I}}$  as the submatrix of  $\mathbf{A}$  with rows and columns indexed by  $\mathcal{I}$ .

If function  $f : \mathbb{R}^n \rightarrow \mathbb{R} \cup \{+\infty\}$  is convex, then the subdifferential of  $f$  at  $\bar{\mathbf{x}}$  is given by  $\partial f(\bar{\mathbf{x}}) := \{\mathbf{z} | f(\bar{\mathbf{x}}) + \langle \mathbf{z}, \mathbf{x} - \bar{\mathbf{x}} \rangle \leq f(\mathbf{x}), \forall \mathbf{x} \in \mathbb{R}^n\}$ . If function  $f$  is lower semi-continuous, then the limiting subdifferential of  $f$  at  $\mathbf{a}$  is given by  $\bar{\partial}f(a) := \{\mathbf{z}^* = \lim_{\mathbf{x}^k \rightarrow \mathbf{a}, f(\mathbf{x}^k) \rightarrow f(\mathbf{a})} z^k, z^k \in \partial_F f(\mathbf{x}^k)\}$ , where  $\partial_F f(\cdot)$  denotes the Frechet subdifferential of  $f$ .

We next recall the notion of first-order stationary points of  $(\mathcal{P})$ .

**Definition 1** (Stationary point [12, Definition 1]). *We say that an  $\mathbf{x}^* \in \mathbb{R}^n$  is a first-stationary point of  $(\mathcal{P})$  if*

$$x_i^* \nabla_i f(\mathbf{x}^*) + \lambda p |x_i^*|^p = 0, \quad \forall i \in [n]. \quad (4)$$

Or equivalently,

$$\nabla_i f(\mathbf{x}^*) + \lambda p |x_i^*|^{p-1} \text{sgn}(x_i^*) = 0, \quad \forall i \in \mathcal{I}(\mathbf{x}^*). \quad (5)$$

The following result is adapted from [12] and states that any local minimizer of  $(\mathcal{P})$  is a stationary point.

**Proposition 2.** *Consider  $(\mathcal{P})$  and let  $\mathbf{x}^*$  be a locally optimal solution. Then  $\mathbf{x}^*$  is a first-order stationary point, implying that (4) is satisfied at  $\mathbf{x}^*$ .*

**Remark 1.** *By (5), we understand that solving for a first-order stationary solution involves identifying its support set. In other words, once the support of the stationary solutions is exactly determined, problem  $(\mathcal{P})$  transforms into a smooth optimization problem.*

Next, we present the first-order stationarity conditions of an approximation problem of  $(\mathcal{P})$ , which is the basis of the proposed algorithm. To overcome the non-smoothness and non-Lipschitz continuity of  $\|\mathbf{x}\|_p$  at some  $x_i = 0$ ,  $\forall i \in [n]$ , we introduce a perturbation parameter  $\epsilon \in \mathbb{R}_{++}^n$  to the  $\ell_p$  regularization term. This modification

results in a smooth and locally Lipschitz continuous objective function, which reads

$$\min_{\mathbf{x} \in \mathbb{R}^n} \quad F(\mathbf{x}; \boldsymbol{\epsilon}) := f(\mathbf{x}) + \lambda \sum_{i=1}^n (|x_i| + \epsilon_i)^p \quad (6)$$

with  $\epsilon_i > 0$ ,  $\forall i \in [n]$ . It is obvious that  $F(\mathbf{x}) = F(\mathbf{x}; \mathbf{0})$ . By [1, Theorem 10.1 & Exercise 8.8(c)], similar to Definition 1, we say that an  $\hat{\mathbf{x}} \in \mathbb{R}^n$  is a first-order stationary point of (6) if

$$0 \in \nabla_i f(\hat{\mathbf{x}}) + \omega_i \partial |\hat{x}_i|, \quad \forall i \in [n], \quad (7)$$

where  $\omega_i := \omega(\hat{x}_i, \epsilon_i) = \lambda p (|\hat{x}_i| + \epsilon_i)^{p-1}$ ,  $\forall i \in [n]$ . An equivalent form of (7) can be written as

$$\begin{aligned} |\nabla_i f(\hat{\mathbf{x}})| &\leq \omega_i, & i \in \mathcal{I}_0(\hat{\mathbf{x}}), \\ \nabla_i f(\hat{\mathbf{x}}) + \omega_i \text{sgn}(\hat{x}_i) &= 0, & i \in \mathcal{I}(\hat{\mathbf{x}}). \end{aligned} \quad (8)$$

The following relationship is revealed between (5) and (7) at  $\mathbf{x}$ . That is,

$$(7) \text{ holds at } \mathbf{x} \text{ and } \epsilon_i = 0, i \in \mathcal{I}(\mathbf{x}) \iff (5) \text{ holds at } \mathbf{x}. \quad (9)$$

## 2 Proposed SOIR $\ell_1$

In this section, we present the proposed second-order iteratively reweighted  $\ell_1$  algorithm for solving  $(\mathcal{P})$ , hereafter referred to SOIR $\ell_1$ , as stated in Algorithm 1. SOIR $\ell_1$  incorporates ideas of subspace acceleration and optimal support identification. It alternates between minimization in a reduced space—determined by the stationarity measures of the zeros and nonzeros in the current solution estimate—and implements iterative soft-thresholding (IST) step during the alternating optimization. The IST step serves both to identify the support of an optimal solution and to ensure the algorithm’s convergence. Whenever the signs of the two successive iterates remain unchanged during iteration, we switch the IST step to an inexact subspace regularized Newton step to enhance convergence. Once the optimal support is identified, SOIR $\ell_1$  then implements a second-order method solely over the nonzeros variables in the support.

### 2.1 Local Weighted $\ell_1$ Regularized Models and Stationarity Measures

Our approach for solving  $(\mathcal{P})$  is partially inspired by the works of [36] and [13]. The basic idea is to exploit the local equivalence between the  $\ell_p$  norm [13, Theorem 9] and the weighted  $\ell_1$  norm. Additionally, we leverage measures of optimality for the  $\ell_1$  regularization convex optimization problem as introduced in FaRSA [36]. Starting with  $\mathbf{x}^k$  at the  $k$ th iteration, we use the concavity of  $|\cdot|_p^p$  over  $\mathbb{R}_{++}$  to form the

---

**Algorithm 1** Proposed SOIR $\ell_1$  for solving  $(\mathcal{P})$ 


---

**Require:**  $(\mathbf{x}^0, \boldsymbol{\epsilon}^0) \in \mathbb{R}^n \times \mathbb{R}_{++}^n$ ,  $\{\eta_\Phi, \eta_\Psi\} \in (0, 1]$ ,  $\{\beta, \xi\} \in (0, 1)$ ,  $\{\bar{\mu}, \gamma, \tau, \alpha, \zeta_0\} \in (0, \infty)$  and  $\varpi \in (0, 1/2]$ .

1: **for**  $k = 0, 1, 2, \dots$  **do**

2:   **while**  $\max\{\|\Psi(\mathbf{x}^k; \boldsymbol{\epsilon}^k)\|, \|\Phi(\mathbf{x}^k; \boldsymbol{\epsilon}^k)\|\} \leq \tau$  **do**

3:     **if**  $\epsilon_i^k \leq \tau, i \in \mathcal{I}^k$  **then**

4:       **return** the (approximate) solution  $\mathbf{x}^k$  of problem  $(\mathcal{P})$ .

5:     **else**

6:       Set  $\epsilon_i^k \in (0, \beta\epsilon_i^k)$ ,  $i \in \mathcal{I}^k$ .

7:     **end if**

8:   **end while**

9:   **if**  $\|\Psi(\mathbf{x}^k; \boldsymbol{\epsilon}^k)\| \geq \gamma\|\Phi(\mathbf{x}^k; \boldsymbol{\epsilon}^k)\|$  **then**

10:     Choose  $\mathcal{W}_k \subseteq \{i : [\Psi(\mathbf{x}^k; \boldsymbol{\epsilon}^k)]_i \neq 0\}$  such that  $\|[\Psi(\mathbf{x}^k; \boldsymbol{\epsilon}^k)]_{\mathcal{W}_k}\| \geq \eta_\Psi\|\Psi(\mathbf{x}^k; \boldsymbol{\epsilon}^k)\|$ .

11:     Call Algorithm 2 to compute  $(\mathbf{x}^{k+1}, \mu^k) \leftarrow \text{IST}(\mathbf{x}^k, \boldsymbol{\omega}^k, \mathcal{W}_k; \alpha, \xi, \bar{\mu})$ .

12:   **else**

13:     Choose  $\mathcal{W}_k \subseteq \{i : [\Phi(\mathbf{x}^k; \boldsymbol{\epsilon}^k)]_i \neq 0\}$  such that  $\|[\Phi(\mathbf{x}^k; \boldsymbol{\epsilon}^k)]_{\mathcal{W}_k}\| \geq \eta_\Phi\|\Phi(\mathbf{x}^k; \boldsymbol{\epsilon}^k)\|$ .

14:     Call Algorithm 2 to compute  $(\hat{\mathbf{x}}^{k+1}, \mu_k) \leftarrow \text{IST}(\mathbf{x}^k, \boldsymbol{\omega}^k, \mathcal{W}_k; \alpha, \xi, \bar{\mu})$ .

15:     **if**  $\text{sgn}(\hat{\mathbf{x}}^{k+1}) = \text{sgn}(\mathbf{x}^k)$  **then**

16:       Set  $\mathbf{H}^k \leftarrow \nabla_{\mathcal{W}_k \mathcal{W}_k}^2 F(\mathbf{x}^k; \boldsymbol{\epsilon}^k) + \zeta_k \mathbf{I} \succ \mathbf{0}$  and  $\mathbf{g}^k \leftarrow \nabla_{\mathcal{W}_k} F(\mathbf{x}^k; \boldsymbol{\epsilon}^k)$ .

17:       Compute a reference direction  $\mathbf{d}_R^k \leftarrow -\frac{\|\mathbf{g}^k\|^2}{\langle \mathbf{g}^k, \mathbf{H}^k \mathbf{g}^k \rangle} \mathbf{g}^k$ .

18:       Compute

$$\mathbf{d}_{\mathcal{W}_k}^k \approx \underset{\mathbf{d} \in \mathbb{R}^{|\mathcal{W}_k|}}{\text{argmin}} \langle \mathbf{g}^k, \mathbf{d} \rangle + \frac{1}{2} \langle \mathbf{d}, \mathbf{H}^k \mathbf{d} \rangle,$$

such that

$$\langle \mathbf{g}^k, \mathbf{d}_{\mathcal{W}_k}^k \rangle \leq \langle \mathbf{g}^k, \mathbf{d}_R^k \rangle \text{ and } m_k(\mathbf{d}_{\mathcal{W}_k}^k) \leq m_k(\mathbf{0}). \quad (10)$$

19:       Set  $\mathbf{d}_{[\mathcal{W}_k]^c}^k = \mathbf{0}$ .

20:       Call Algorithm 3 to compute  $(\mathbf{x}^{k+1}, \mu^k) \leftarrow \text{PLS}(\mathbf{x}^k; \boldsymbol{\epsilon}^k, \mathbf{d}^k, \mathcal{W}_k; \varpi, \xi)$ .

21:     **else**

22:       Set  $\mathbf{x}^{k+1} \leftarrow \hat{\mathbf{x}}^{k+1}$ .

23:     **end if**

24:   **end if**

25:   Update  $\epsilon_i^{k+1} \in (0, \beta\epsilon_i^k)$ ,  $i \in \mathcal{I}^{k+1}$ .

26:   Update  $\omega_i^{k+1} = \lambda p(|x_i^{k+1}| + \epsilon_i^{k+1})^{p-1}$ ,  $i \in [n]$ .

27: **end for**

---

following locally weighted  $\ell_1$  regularized minimization model:

$$\min_{\mathbf{x} \in \mathbb{R}^n} G_k(\mathbf{x}) = f(\mathbf{x}) + \sum_{i=1}^n \omega_i^k |x_i|, \quad (11)$$

where  $\omega_i^k = \lambda p(|x_i^k| + \epsilon_i^k)^{p-1}$ ,  $\forall i \in [n]$ . By [1, Theorem 10.1 & Exercise 8.8(c)], similar to Definition 1, we say that an  $\mathbf{x} \in \mathbb{R}^n$  is a first-order stationary point of problem (11) if

$$0 \in \nabla_i f(\mathbf{x}) + \omega_i^k \partial|x_i|, \quad \forall i \in [n]. \quad (12)$$

The following lemma reveals a relationship in terms of the stationarity at a solution estimate between the locally approximated model  $G_k(\mathbf{x})$  and the perturbed  $F(\mathbf{x}; \boldsymbol{\epsilon}^k)$ .

**Lemma 1.** *Consider (6) and (11). The following statements are equivalent:*

- (i)  $\mathbf{x}$  is first-order stationary for (11).
- (ii)  $\mathbf{x}$  is first-order stationary for (6) with  $\boldsymbol{\epsilon} = \boldsymbol{\epsilon}^k$ .
- (iii)  $\mathbf{x} = \mathbb{S}_{\boldsymbol{\omega}^k}(\mathbf{x} - \nabla f(\mathbf{x}))$ .

*Proof.* The statement holds true by noting that

$$\begin{aligned} (i) \xrightarrow{(12)} \quad -\nabla f(\mathbf{x}) &\in \langle \boldsymbol{\omega}^k, \partial\|\mathbf{x}\|_1 \rangle \iff (\mathbf{x} + \langle \boldsymbol{\omega}^k, \partial\|\mathbf{x}\|_1 \rangle) \ni (\mathbf{x} - \nabla f(\mathbf{x})) \\ \iff (iii) \iff (7) \text{ is satisfied} &\iff (ii). \end{aligned} \quad (13)$$

This completes the proof.  $\square$

Let  $(\mathbf{x}, \boldsymbol{\epsilon})$  be a solution estimate. For ease of presentation, define the following index sets:

$$\begin{aligned} \kappa_1(\mathbf{x}) &= \{i \in [n] \mid \nabla_i f(\mathbf{x}) + \omega_i < 0\}, \quad \kappa_2(\mathbf{x}) = \{i \in [n] \mid \nabla_i f(\mathbf{x}) - \omega_i > 0\}, \\ \kappa_3(\mathbf{x}) &= \{i \in [n] \mid \nabla_i f(\mathbf{x}) + \omega_i > 0\}, \quad \kappa_4(\mathbf{x}) = \{i \in [n] \mid \nabla_i f(\mathbf{x}) - \omega_i < 0\}. \end{aligned}$$

We also define two stationarity residuals,  $\Psi(\mathbf{x}; \boldsymbol{\epsilon})$  and  $\Phi(\mathbf{x}; \boldsymbol{\epsilon})$ , corresponding to zeros and nonzeros at  $(\mathbf{x}; \boldsymbol{\epsilon})$ , respectively. That is,

$$[\Psi(\mathbf{x}; \boldsymbol{\epsilon})]_i := \begin{cases} \nabla_i f(\mathbf{x}) + \omega_i, & \text{if } i \in \mathcal{I}_0(\mathbf{x}) \cap \kappa_1(\mathbf{x}), \\ \nabla_i f(\mathbf{x}) - \omega_i, & \text{if } i \in \mathcal{I}_0(\mathbf{x}) \cap \kappa_2(\mathbf{x}), \\ 0, & \text{otherwise;} \end{cases} \quad (14)$$

and

$$[\Phi(\mathbf{x}; \boldsymbol{\epsilon})]_i := \begin{cases} 0, & \text{if } i \in \mathcal{I}_0(\mathbf{x}), \\ \min\{\nabla_i f(\mathbf{x}) + \omega_i, \max\{x_i, \nabla_i f(\mathbf{x}) - \omega_i\}\}, & \text{if } i \in \mathcal{I}_+(\mathbf{x}) \cap \kappa_3(\mathbf{x}), \\ \max\{\nabla_i f(\mathbf{x}) - \omega_i, \min\{x_i, \nabla_i f(\mathbf{x}) + \omega_i\}\}, & \text{if } i \in \mathcal{I}_-(\mathbf{x}) \cap \kappa_4(\mathbf{x}), \\ \nabla_i f(\mathbf{x}) + \omega_i \cdot \text{sgn}(x_i), & \text{otherwise.} \end{cases} \quad (15)$$

We provide some intuitive arguments on the defined stationarity residuals.

**Remark 2.** *Consider that if the stationarity condition (8) holds at  $(\mathbf{x}; \boldsymbol{\epsilon})$ , then  $|\nabla_i f(\mathbf{x})| \leq \omega_i$  for any  $i \in \mathcal{I}_0(\mathbf{x})$ . This indicates that  $|[\Psi(\mathbf{x}; \boldsymbol{\epsilon})]_i|$  reflects how close the zero components are to being stationary for (6). For  $i \in \mathcal{I}_+(\mathbf{x}) \cup \mathcal{I}_-(\mathbf{x})$ , the stationarity condition (8) results in  $\nabla_i f(\mathbf{x}) + \omega_i \cdot \text{sgn}(x_i) = 0$ . Thus,  $|[\Phi(\mathbf{x}; \boldsymbol{\epsilon})]_i|$  indicates how close the nonzero components are being to stationary for (6). Additionally, the stationarity residual  $[\Phi(\mathbf{x}; \boldsymbol{\epsilon})]_i$  measures the distance that a nonzero component may shift before it becomes zero.*

**Remark 3.** The defined stationarity residuals for zero and nonzero components motivate the development of a subspace method that minimizes different sets of variables at each iteration. In the proposed algorithm, these residuals serve as the “switching mechanism” for optimizing zero versus nonzero components. If  $\|\Psi(\mathbf{x}, \boldsymbol{\epsilon})\| \geq \gamma \|\Phi(\mathbf{x}, \boldsymbol{\epsilon})\|$  for some prescribed  $\gamma \in (0, +\infty)$ , it suggests that the zero components of  $\mathbf{x}$  have a relatively greater impact on the stationarity residual than the nonzero components. Consequently, we perform the minimization in the reduced space  $\mathbb{R}^{|\mathcal{W}|}$  with  $\mathcal{W} \subseteq \{i : [\Psi(\mathbf{x}, \boldsymbol{\epsilon})]_i \neq 0\}$  such that  $\|[\Psi(\mathbf{x}, \boldsymbol{\epsilon})]_{\mathcal{W}}\| \geq \eta_{\Psi} \|\Psi(\mathbf{x}, \boldsymbol{\epsilon})\|$  with  $\eta_{\Psi} \in (0, 1)$ . Conversely, if  $\|\Psi(\mathbf{x}, \boldsymbol{\epsilon})\| < \gamma \|\Phi(\mathbf{x}, \boldsymbol{\epsilon})\|$ , it indicates that the nonzero components of  $\mathbf{x}$  have a relatively greater impact on the stationarity residual than the zero components. In this case, we perform the minimization in the reduced space  $\mathbb{R}^{|\mathcal{W}|}$  with  $\mathcal{W} \subseteq \{i : [\Phi(\mathbf{x}, \boldsymbol{\epsilon})]_i \neq 0\}$  such that  $\|[\Phi(\mathbf{x}, \boldsymbol{\epsilon})]_{\mathcal{W}}\| \geq \eta_{\Phi} \|\Phi(\mathbf{x}, \boldsymbol{\epsilon})\|$  with  $\eta_{\Phi} \in (0, 1)$ . A detailed discussion of this approach is presented in the subsequent sections.

The following lemma provides a formal understanding of stationarity measures (14) and (15).

**Proposition 3.** Consider (14) and (15). The following statements hold.

(i) For any  $(\mathbf{x}; \boldsymbol{\epsilon})$  with  $\boldsymbol{\epsilon} \in \mathbb{R}_{++}^n$  and  $\boldsymbol{\omega} = \boldsymbol{\omega}(\mathbf{x}; \boldsymbol{\epsilon})$ , it holds that

$$|[\Phi(\mathbf{x}; \boldsymbol{\epsilon})]_i| \leq |\nabla_i F(\mathbf{x}; \boldsymbol{\epsilon})|, \quad i \in \mathcal{I}(\mathbf{x}). \quad (16)$$

(ii) Let  $d(\mu) := \mathbb{S}_{\mu\boldsymbol{\omega}}(\mathbf{x} - \mu \nabla f(\mathbf{x})) - \mathbf{x}$  for  $\mu > 0$ , the following decomposition holds:

$$d(1) = -[\Psi(\mathbf{x}; \boldsymbol{\epsilon}) + \Phi(\mathbf{x}; \boldsymbol{\epsilon})]. \quad (17)$$

More generally,

$$d_i(\mu) = -\mu [\Psi(\mathbf{x}; \boldsymbol{\epsilon})]_i, \quad i \in \mathcal{I}_0(\mathbf{x}), \quad (18a)$$

$$|d_i(\mu)| \geq \min\{\mu, 1\} |[\Phi(\mathbf{x}; \boldsymbol{\epsilon})]_i|, \quad i \in \mathcal{I}(\mathbf{x}). \quad (18b)$$

(iii)  $\mathbf{x}$  satisfies the first-order stationarity condition (8) if

$$\|\Phi(\mathbf{x}; \boldsymbol{\epsilon})\| = \|\Psi(\mathbf{x}; \boldsymbol{\epsilon})\| = 0. \quad (19)$$

Additionally, if  $\epsilon_i = 0$  for  $i \in \mathcal{I}(\mathbf{x})$ , then (19) implies that  $\mathbf{x}$  satisfies the first-order stationarity condition (5).

(iv) Suppose  $\|\Phi(\mathbf{x}; \boldsymbol{\epsilon})\| \neq 0$  and  $\|\Psi(\mathbf{x}; \boldsymbol{\epsilon})\| \neq 0$ . Then  $\mathcal{W}_{\Phi} \subseteq \{i : [\Phi(\mathbf{x}; \boldsymbol{\epsilon})]_i \neq 0\} \subseteq \mathcal{I}(\mathbf{x})$  or  $\mathcal{W}_{\Psi} \subseteq \{i : [\Psi(\mathbf{x}; \boldsymbol{\epsilon})]_i \neq 0\} \subseteq \mathcal{I}_0(\mathbf{x})$  are nonempty.

*Proof.* (i) We consider the last three cases presented in (15). For  $i \in \mathcal{I}_+(\mathbf{x})$ , we have  $\nabla_i F(\mathbf{x}; \boldsymbol{\epsilon}) = \nabla_i f(\mathbf{x}) + \omega_i$  by (8). When  $i \in \mathcal{I}_+(\mathbf{x}) \cap \kappa_3(\mathbf{x})$ , we also have that  $[\Phi(\mathbf{x}; \boldsymbol{\epsilon})]_i = \min\{\nabla_i f(\mathbf{x}) + \omega_i, x_i\} \leq \nabla_i f(\mathbf{x}) + \omega_i$  if  $\nabla_i f(\mathbf{x}) - \omega_i < 0$ , and otherwise  $[\Phi(\mathbf{x}; \boldsymbol{\epsilon})]_i = \min\{\nabla_i f(\mathbf{x}) + \omega_i, \nabla_i f(\mathbf{x}) - \omega_i\} \leq \nabla_i f(\mathbf{x}) + \omega_i$ . As for the last case, it is obvious that  $[\Phi(\mathbf{x}; \boldsymbol{\epsilon})]_i = \nabla_i f(\mathbf{x}) + \omega_i = \nabla_i F(\mathbf{x}; \boldsymbol{\epsilon})$ . On the other hand, similar arguments can be applied when  $i \in \mathcal{I}_-(\mathbf{x}) \cap \kappa_4(\mathbf{x})$ . Overall, we have shown that (16) holds.

(ii) The proof of (17) can be found in [36, Lemma A.1]. It indicates that  $\Psi(\mathbf{x}; \boldsymbol{\epsilon}) = -d_i(1)$ ,  $i \in \mathcal{I}_0(\mathbf{x})$  and  $\Phi(\mathbf{x}; \boldsymbol{\epsilon}) = -d_i(1)$ ,  $i \in \mathcal{I}(\mathbf{x})$  by the complementarity of  $\Psi$  and  $\Phi$ . This, together with Lemma A shown in Appendix, implies (18a) and (18b).

(iii) If (19) is satisfied, then (8) holds by (17) and (13). Moreover, if  $\epsilon_i = 0$ ,  $i \in \mathcal{I}(\mathbf{x})$ , it follows from (9) that  $\mathbf{x}$  satisfies the first-order stationarity condition (5).

(iv) Obvious. This completes the proof of all statements.  $\square$

Proposition 3(iii) implies a practical termination condition for the proposed algorithm. Specifically, when  $\max\{\|\Psi(\mathbf{x}; \boldsymbol{\epsilon})\|, \|\Phi(\mathbf{x}; \boldsymbol{\epsilon})\|\}$  and  $\epsilon_i, i \in \mathcal{I}(\mathbf{x})$  are relatively small, the solution estimate  $\mathbf{x}$  is nearly a stationary point of  $(\mathcal{P})$ . This proposition also informs the updating strategy for  $\boldsymbol{\epsilon} \in \mathbb{R}_{++}^n$ . A reasonable updating strategy should rapidly drive  $\epsilon_i$ ,  $i \in [n]$  associated with the nonzeros of  $\mathbf{x}$ , to zero once the correct support  $\mathcal{I}(\mathbf{x})$  is identified. Meanwhile,  $\epsilon_i$ ,  $i \in \mathcal{I}_0(\mathbf{x})$  should be fixed as constants [13]. The key idea behind this strategy is to eliminate the zeros and the associated  $\epsilon_i$  from  $F(\mathbf{x}; \boldsymbol{\epsilon})$ , thereby transforming the problem into a smooth one. This transformation is crucial for the convergence analysis. In SOIR $\ell_1$ , we only decrease  $\epsilon_i$ ,  $i \in [n]$  associated with the nonzeros of  $\mathbf{x}$  (Lines 6 and 25 of Algorithm 1).

## 2.2 Reduced-space Proximal Weighted $\ell_1$ Regularized Subproblem

The sequence generated by SOIR $\ell_1$  consists of solution estimates obtained either by solving subspace proximal first-order approximate subproblems or by solving subspace regularized Newton subproblems. To correctly identify the support of a desired stationary point and ensure global convergence, we construct an approximate model of (11) by replacing the function  $f$  with its locally linear approximation and a proximal term while retaining the weighted  $\ell_1$ -norm restricted to a subset of the nonzero variables (refer to Lines 11 and 14 of Algorithm 1), i.e.,

$$\min_{\mathbf{x}_{\mathcal{W}} \in \mathbb{R}^{|\mathcal{W}|}} Q_{\mu_k}(\mathbf{x}_{\mathcal{W}}; \mathbf{x}^k) := \langle \nabla_{\mathcal{W}} f(\mathbf{x}^k), \mathbf{x}_{\mathcal{W}} \rangle + \frac{1}{2\mu_k} \|\mathbf{x}_{\mathcal{W}} - \mathbf{x}_{\mathcal{W}}^k\|_2^2 + \sum_{i \in \mathcal{W}} \omega_i^k |x_i|, \quad (20)$$

where  $\mathcal{W} \subset [n]$  is formed according to the relative impact of zeros and nonzeros of the current iterate and  $\mu_k > 0$ . The formed subproblem highlights a notable difference between SOIR $\ell_1$  and HpgSRN [33]. The subproblem (20) admits a closed-form solution  $\mathbf{x}_{\mathcal{W}}^* = [\mathbb{S}_{\mu_k}(\mathbf{x}^k - \mu_k \nabla f(\mathbf{x}^k))]_{\mathcal{W}}$  in a low-dimensional space  $\mathbb{R}^{|\mathcal{W}|}$ , which can be efficiently computed. In contrast, HpgSRN requires a proximal gradient method to solve the subproblem in the full  $n$ -dimensional space iteratively. To ensure global convergence, we use a simple variant of the inexact line-search with backtracking to find a proper value of  $\mu_k$  such that  $G_k(\mathbf{x}^j) \leq G_k(\mathbf{x}) - \frac{\alpha}{2} \|\mathbf{x}^j - \mathbf{x}\|^2$  is satisfied, where  $\mathbf{x}^j$  a solution estimate in the  $j$ th iteration of Algorithm 2 and  $\alpha > 0$  is a prescribed scalar.

For ease of presentation, we drop the iteration counter superscript  $k$  in the outer loop in Algorithm 2. The following lemma proves that the line-search with backtracking, as described in Lines 2–8 of Algorithm 2, terminates in a finite number of steps.

---

**Algorithm 2** IST step:  $[\mathbf{x}^j, \mu_j] := \text{IST}(\mathbf{x}, \boldsymbol{\omega}, \mathcal{W}; \alpha, \xi, \bar{\mu})$ 


---

**Require:**  $\{\mathbf{x}, \boldsymbol{\omega}\} \in \mathbb{R}^n$ ,  $\mathcal{W} \subseteq [n]$ ;  $\{\bar{\mu}, \alpha\} \in (0, +\infty)$  and  $\xi \in (0, 1)$ .

```

1: Let  $\mu_0 \leftarrow \bar{\mu}$  and  $\mathbf{x}_{\mathcal{W}^c}^0 \leftarrow \mathbf{x}_{\mathcal{W}^c}$ ,  $\mathbf{x}_{\mathcal{W}}^0 \leftarrow [\mathbb{S}_{\mu_0 \boldsymbol{\omega}}(\mathbf{x} - \mu^0 \nabla f(\mathbf{x}))]_{\mathcal{W}}$ .
2: for  $j = 0, 1, 2, \dots$  do
3:   if  $G_k(\mathbf{x}^j) \leq G_k(\mathbf{x}) - \frac{\alpha}{2} \|\mathbf{x}^j - \mathbf{x}\|^2$  then
4:     return  $\mathbf{x}^j$ .
5:   end if
6:    $\mu_{j+1} \leftarrow \xi \mu_j$ .
7:    $\mathbf{x}_{\mathcal{W}^c}^{j+1} \leftarrow \mathbf{x}_{\mathcal{W}^c}$ ,  $\mathbf{x}_{\mathcal{W}}^{j+1} \leftarrow [\mathbb{S}_{\mu_{j+1} \boldsymbol{\omega}}(\mathbf{x} - \mu_{j+1} \nabla f(\mathbf{x}))]_{\mathcal{W}}$ .
8: end for

```

---

**Lemma 2.** Suppose Algorithm 2 is invoked with  $(\hat{\mathbf{x}}, \hat{\mu}) = \text{IST}(\mathbf{x}, \boldsymbol{\omega}, \mathcal{W}; \alpha, \xi, \bar{\mu})$ . Then Algorithm 2 determines in a finite number of iterations a value  $\hat{\mu}$  that satisfies the condition of the Line 3 of Algorithm 2. Moreover, for  $L_1(\mathbf{x}) > 0$ , we have

$$\min\{\bar{\mu}, \frac{\xi}{L_1(\mathbf{x}) + \alpha}\} \leq \hat{\mu} \leq \bar{\mu} \quad (21)$$

and

$$F(\hat{\mathbf{x}}; \epsilon) - F(\mathbf{x}, \epsilon) \leq -\frac{\alpha}{2} \|\hat{\mathbf{x}} - \mathbf{x}\|^2. \quad (22)$$

*Proof.* We first provide some local properties on the function  $\nabla f$  restricted to a reduced space  $\mathbb{R}^{|\mathcal{W}|}$ . For each  $j \in \mathbb{N}$ , we have from  $\mu_j \leq \bar{\mu}$  (see Line 6) and  $\mathbf{x}_{\mathcal{W}}^j = [\mathbb{S}_{\mu_j \boldsymbol{\omega}}(\mathbf{x} - \mu_j \nabla f(\mathbf{x}))]_{\mathcal{W}}$  and  $\mathbf{x}_{\mathcal{W}^c}^j = \mathbf{x}_{\mathcal{W}^c}$  that

$$\begin{aligned} Q_{\bar{\mu}}(\mathbf{x}_{\mathcal{W}}^j; \mathbf{x}) &\leq \langle \nabla_{\mathcal{W}} f(\mathbf{x}), \mathbf{x}_{\mathcal{W}}^j \rangle + \frac{1}{2\mu_j} \|\mathbf{x}_{\mathcal{W}} - \mathbf{x}_{\mathcal{W}}^j\|_2^2 + \sum_{i \in \mathcal{W}} \omega_i |x_i^j| \\ &\leq \sum_{i \in \mathcal{W}} \omega_i |x_i| = Q_{\bar{\mu}}(\mathbf{x}_{\mathcal{W}}; \mathbf{x}). \end{aligned} \quad (23)$$

Since  $Q_{\bar{\mu}}(\cdot; \mathbf{x})$  is continuous and coercive, we know that the level set  $\text{Lev}_{Q_{\bar{\mu}}(\cdot; \mathbf{x})} := \{\mathbf{z} \in \mathbb{R}^{|\mathcal{W}|} \mid Q_{\bar{\mu}}(\mathbf{z}; \mathbf{x}) \leq Q_{\bar{\mu}}(\mathbf{x}_{\mathcal{W}}; \mathbf{x})\}$  is compact. Additionally, since  $\nabla_{\mathcal{W}} f$  is continuously differentiable, we know that there exists  $L_1(\mathbf{x})$  such that for any  $\mathbf{y}, \mathbf{z} \in \text{Lev}_{Q_{\bar{\mu}}(\cdot; \mathbf{x})}$ ,

$$\|\nabla_{\mathcal{W}} f(\mathbf{y}) - \nabla_{\mathcal{W}} f(\mathbf{z})\| \leq L_1(\mathbf{x}) \|\mathbf{y} - \mathbf{z}\|. \quad (24)$$

We now prove the statement by seeking a contradiction. Suppose Algorithm 2 with backtracking cycles indefinitely between Line 3 and 7. Then Line 3 of Algorithm 2 is never implemented, and hence for any trial point  $\mathbf{x}^j$  with  $j \in \mathbb{N}$ , it holds that

$$G(\mathbf{x}^j) > G(\mathbf{x}) - \frac{\alpha}{2} \|\mathbf{x}^j - \mathbf{x}\|^2. \quad (25)$$

Note however that  $\xi \in (0, 1)$  and  $\mu_j \rightarrow 0$  as  $j \rightarrow +\infty$  and therefore, for  $j \rightarrow +\infty$   $\mathbf{x}_{\mathcal{W}}^j = [\mathbb{S}_{\mu_j \boldsymbol{\omega}}(\mathbf{x} - \mu_j \nabla f(\mathbf{x}))]_{\mathcal{W}} \rightarrow \mathbf{x}_{\mathcal{W}}$  by noting that  $\nabla_{\mathcal{W}} f(\mathbf{x})$  is bounded over  $\text{Lev}_{Q_{\bar{\mu}}(\cdot; \mathbf{x})}$ .

This, together with the continuity of  $G(\cdot)$  and  $\|\cdot\|^2$ , gives  $\lim_{j \rightarrow +\infty} G(\mathbf{x}^j) = G(\mathbf{x})$  and  $\|\mathbf{x}^j - \mathbf{x}\|^2 \rightarrow 0$ . By (25), the contradiction  $0 > 0$  shows that the exists a finite  $j_0$  such that  $G(\mathbf{x}^{j_0}) \leq G(\mathbf{x}) - \frac{\alpha}{2}\|\mathbf{x}^j - \mathbf{x}\|^2$ . Then it follows from (24) and (23) that for any  $\mu_j \leq \frac{1}{L_1(\mathbf{x}) + \alpha}$ ,

$$\begin{aligned} G(\mathbf{x}^j) &\leq f(\mathbf{x}) + \langle \nabla f(\mathbf{x}), \mathbf{x}^j - \mathbf{x} \rangle + \frac{L_1(\mathbf{x})}{2}\|\mathbf{x}^j - \mathbf{x}\|^2 + \sum_{i=1}^n \omega_i |x_i^j| \\ &\leq f(\mathbf{x}) + \langle \nabla f(\mathbf{x}), \mathbf{x}^j - \mathbf{x} \rangle + \frac{1}{2\mu_j}\|\mathbf{x}^j - \mathbf{x}\|^2 + \sum_{i=1}^n \omega_i |x_i^j| - \frac{\alpha}{2}\|\mathbf{x}^j - \mathbf{x}\|^2 \quad (26) \\ &\leq f(\mathbf{x}) + \sum_{i=1}^n \omega_i |x_i| - \frac{\alpha}{2}\|\mathbf{x}^j - \mathbf{x}\|^2 = G(\mathbf{x}) - \frac{\alpha}{2}\|\mathbf{x}^j - \mathbf{x}\|^2. \end{aligned}$$

Therefore, we have  $\min\{\bar{\mu}, \frac{\xi}{L_1(\mathbf{x}) + \alpha}\} \leq \mu_{j_0} \leq \bar{\mu}$ . Denote  $\hat{\mathbf{x}} = \mathbf{x}^{j_0}$ . It follows from the concavity of  $|\cdot|^p$  over  $\mathbb{R}_{++}$  that  $\lambda[(|\hat{x}_i| + \epsilon_i)^p - (|x_i| + \epsilon_i)^p] \leq \omega_i(|\hat{x}_i| - |x_i|)$ . Then, it holds that

$$F(\hat{\mathbf{x}}; \boldsymbol{\epsilon}) - F(\mathbf{x}, \boldsymbol{\epsilon}) \leq G(\hat{\mathbf{x}}; \boldsymbol{\epsilon}) - G(\mathbf{x}, \boldsymbol{\epsilon}). \quad (27)$$

This, together with (26), gives (22). The proof is complete.  $\square$

In the following lemma, we demonstrate some useful properties regarding the support of the  $k$ -th iterate when the Algorithm 2 is invoked.

**Lemma 3.** *Consider Algorithm 1. Suppose the termination criterion of Algorithm 1 is not satisfied. Then the following hold.*

- (i) *If  $\|\Psi(\mathbf{x}^k; \boldsymbol{\epsilon}^k)\| \geq \gamma\|\Phi(\mathbf{x}^k; \boldsymbol{\epsilon}^k)\|$  and Lines 10 and 11 are executed. Then  $\mathcal{I}^k \subseteq \mathcal{I}^{k+1}$ . Indeed, it holds that  $\mathcal{I}^{k+1} = \mathcal{I}^k \cup \mathcal{W}_k$  and  $|\mathcal{I}^{k+1}| = |\mathcal{I}^k| + |\mathcal{W}_k|$ .*
- (ii) *If  $\|\Psi(\mathbf{x}^k; \boldsymbol{\epsilon}^k)\| < \gamma\|\Phi(\mathbf{x}^k; \boldsymbol{\epsilon}^k)\|$  and Lines 13 and 14 are executed, but Line 15 is not triggered. Then  $\mathcal{I}^k \supset \mathcal{I}^{k+1}$ .*

*Proof.* (i). Suppose  $\|\Psi(\mathbf{x}^k; \boldsymbol{\epsilon}^k)\| \geq \gamma\|\Phi(\mathbf{x}^k; \boldsymbol{\epsilon}^k)\|$ . Then

$$\emptyset \neq \mathcal{W}_k \subseteq \{i : [\Psi(\mathbf{x}^k; \boldsymbol{\epsilon}^k)]_i \neq 0\} \subseteq \mathcal{I}_0^k \quad (28)$$

is chosen (see Line 10) such that the norm of  $\Psi(\mathbf{x}^k; \boldsymbol{\epsilon}^k)$  over  $\mathcal{W}_k$  is greater than a fraction of  $\Psi(\mathbf{x}^k; \boldsymbol{\epsilon}^k)$  over all components, and SOIR $\ell_1$  calls the subroutine IST step (see Line 11) in the reduced space  $\mathbb{R}^{|\mathcal{W}_k|}$  and gives a solution estimate  $\mathbf{x}^{k+1}$ . We therefore conclude that  $\mathcal{I}^k \subseteq \mathcal{I}^{k+1}$ , meaning zero components could become nonzero in this step. In fact, by Proposition 3(ii) and (28), we have

$$x_i^{k+1} - x_i^k = \mu_k [\Psi(\mathbf{x}^k; \boldsymbol{\epsilon}^k)]_i \neq 0, i \in \mathcal{W}_k.$$

Then, we know  $\mathcal{I}^{k+1} = \mathcal{I}^k \cup \mathcal{W}_k$  and  $\mathcal{I}^k \cap \mathcal{W}_k = \emptyset$ . Hence,  $|\mathcal{I}^{k+1}| = |\mathcal{I}^k| + |\mathcal{W}_k|$ .

(ii). Suppose  $\|\Psi(\mathbf{x}^k; \boldsymbol{\epsilon}^k)\| < \gamma\|\Phi(\mathbf{x}^k; \boldsymbol{\epsilon}^k)\|$ . Then

$$\emptyset \neq \mathcal{W}_k \subseteq \{i : \Phi_i^k \neq 0\} \subseteq \mathcal{I}^k$$

is chosen (see Line 13) such that the norm of  $\Phi^k$  over this subset is greater than a fraction of  $\Phi^k$  over all components, SOIR $\ell_1$  calls the subroutine IST step (see Line 14) in the reduced space  $\mathbb{R}^{|\mathcal{W}_k|}$  and gives a solution estimate  $\hat{\mathbf{x}}^{k+1}$ . If  $\text{sign}(\hat{\mathbf{x}}^{k+1}) \neq \text{sign}(\mathbf{x}^k)$  (see Line 15), then  $\hat{\mathbf{x}}^{k+1}$  is accepted as the new iterate (see Line 22). We then conclude that  $\mathcal{I}^k \supset \mathcal{I}^{k+1}$ , meaning that zero components could become nonzeros in this step. This completes the proof.  $\square$

### 2.3 Reduced-space Quadratic Subproblems

In [13, Theorem 4], the authors showed that the IR $\ell_1$  algorithm has a locally stable sign property, meaning the sign of its sequence remains fixed after a certain number of iterations. This property follows naturally from the stable support property [13, Theorem 3]. Once the support is identified, a more efficient second-order method can be applied to the nonzero elements to speed up local convergence. However, it is generally not possible to know in advance if the support has been identified. To address this, when two successive iterates,  $\mathbf{x}^k$  and  $\hat{\mathbf{x}}^{k+1}$ , share the same sign (see Line 15), SOIR $\ell_1$  minimizes a quadratic subproblem restricted to a subset of nonzero variables (Lines 16–19), which reads

$$\min_{\mathbf{d} \in \mathbb{R}^{|\mathcal{W}_k|}} m_k(\mathbf{d}) := \langle \mathbf{g}^k, \mathbf{d} \rangle + \frac{1}{2} \langle \mathbf{d}, \mathbf{H}^k \mathbf{d} \rangle, \quad (29)$$

where  $\mathbf{g}^k = \nabla_{\mathcal{W}_k} F(\mathbf{x}^k; \boldsymbol{\epsilon}^k)$  is the subspace gradient of  $F(\mathbf{x}^k; \boldsymbol{\epsilon}^k)$  and  $\mathbf{H}^k = \nabla_{\mathcal{W}_k \mathcal{W}_k}^2 F(\mathbf{x}^k; \boldsymbol{\epsilon}^k) + \zeta \mathbf{I} \succ \mathbf{0}$  is a modified subspace Hessian matrix related to  $F(\mathbf{x}^k; \boldsymbol{\epsilon}^k)$  with  $\zeta_k \in (0, +\infty)$ . Since the working index set  $\mathcal{W}_k \subseteq \mathcal{I}(\mathbf{x}^k)$  is nonempty by Proposition 3, the objective function  $F(\mathbf{x}; \boldsymbol{\epsilon})$  is smooth with respect to the variables restricted to  $\mathcal{W}_k$  at  $\mathbf{x}^k$ .

Since the local quadratic model  $m_k$  is constructed in the reduced space  $\mathbb{R}^{|\mathcal{W}_k|}$ , it often has a relatively small dimension. Consequently, problem (29) can be efficiently solved using many existing quadratic programming methods, such as the Conjugate Gradient (CG) method [37]. It is worth noting that SOIR $\ell_1$  is independent of the choice of the subproblem solver.

When the correct support of an optimal solution is detected, an exact reduced-space Hessian of the objective function  $F$  is employed in the neighborhood of the optimization point, causing the algorithm to revert to a classic Newton method. Otherwise, the unboundedness of  $\mathbf{H}^k$  should be addressed. One simple technique is given by the Levenberg-Marquardt method, which modifies the Hessian by adding a multiple of identity matrix to ensure positive definiteness and hence yield a descent search direction. Another technique is to consider a trust region for the search direction to avoid unboundedness, typically requiring a tailored solver to find the (global) optimal solution of the subproblem. This discussion will be deferred to a subsequent section.

It should be noted that the subproblem solver does not require an exact minimizer of  $m_k$  to be found during each iteration. Let  $\mathbf{d}_R^k$  be a reference direction, computed by minimizing  $m_k$  along the steepest descent direction (see Line 17). We permit an inexact solution estimate of (29) as long as the solution  $\mathbf{d}_{\mathcal{W}_k}^k$  results in a reduction of the objective  $m_k$  and is more effective than  $\mathbf{d}_R^k$  (see Line 18). Specifically,  $m_k(\mathbf{d}_{\mathcal{W}_k}^k) \leq$

$m_k(\mathbf{0})$  and  $\langle \mathbf{g}^k, \mathbf{d}_{\mathcal{W}_k}^k \rangle \leq \langle \mathbf{g}^k, \mathbf{d}_R^k \rangle$ . We use  $\mathbf{d}_{\mathcal{W}_k}^k$  and  $\mathbf{d}_{[\mathcal{W}_k]^c}^k = \mathbf{0}$  to update the search direction  $\mathbf{d}^k \in \mathbb{R}^n$  accordingly (see Line 19).

**Assumption 4.** For  $\mathbf{H}^k \succ \mathbf{0}$  obtained from the Line 16 of Algorithm 1,  $\mathbf{H}^k$  is bounded and uniformly positive definite, i.e., there exist  $0 < \bar{\lambda}_{\min} < \bar{\lambda}_{\max} < +\infty$  such that

$$\bar{\lambda}_{\min} \|\mathbf{z}\|^2 \leq \langle \mathbf{z}, \mathbf{H}^k \mathbf{z} \rangle \leq \bar{\lambda}_{\max} \|\mathbf{z}\|^2, \quad \forall \mathbf{z} \in \mathbb{R}^{|\mathcal{W}_k|}. \quad (30)$$

After obtaining an inexact solution of the reduced QP subproblem (29), we achieve the following result.

**Lemma 4.** Consider the reduced-space QP subproblem (29) with  $\mathbf{H}^k \succ \mathbf{0}$ . Then the following inequalities hold.

$$\langle \mathbf{g}^k, \mathbf{d}_{\mathcal{W}_k}^k \rangle \leq \langle \mathbf{g}^k, \mathbf{d}_R^k \rangle < 0, \quad (31)$$

$$|\langle \mathbf{g}^k, \mathbf{d}_{\mathcal{W}_k}^k \rangle| \geq |\langle \mathbf{g}^k, \mathbf{d}_R^k \rangle| = \frac{\|\mathbf{g}^k\|^2}{\langle \mathbf{g}^k, \mathbf{H}^k \mathbf{g}^k \rangle} \|\mathbf{g}^k\|^2 \geq \frac{\|\mathbf{g}^k\|^2}{\bar{\lambda}_{\max}}, \quad (32)$$

$$\frac{\|\mathbf{g}^k\|}{\bar{\lambda}_{\max}} \leq \|\mathbf{d}_{\mathcal{W}_k}^k\| \leq \frac{2\|\mathbf{g}^k\|}{\bar{\lambda}_{\min}}. \quad (33)$$

*Proof.* Inequalities (31) and (32) can be easily verified mainly by the definition of  $\mathbf{d}_R^k$ . We therefore only prove (33). Let  $\mathbf{d}_N^k$  denote the exact solution (29). We know from the optimality condition of (29) that

$$\mathbf{H}^k \mathbf{d}_N^k = -\mathbf{g}^k. \quad (34)$$

It follows that

$$\|\mathbf{d}_N^k\| = \|(\mathbf{H}^k)^{-1}\| \|\mathbf{g}^k\| \leq \frac{\|\mathbf{g}^k\|}{\bar{\lambda}_{\min}}. \quad (35)$$

Define a quadratic function  $\bar{m}_k(\mathbf{d}) := m_k(\mathbf{d}_N^k + \mathbf{d})$  and the associated level set  $\text{Lev}_{\bar{m}_k} := \{\mathbf{d} \in \mathbb{R}^{|\mathcal{W}_k|} \mid \bar{m}_k(\mathbf{d}) \leq 0\}$ . We then see that

$$(\mathbf{d}_{\mathcal{W}_k}^k - \mathbf{d}_N^k) \in \text{Lev}_{\bar{m}_k}, \quad (36)$$

since  $\bar{m}_k(\mathbf{d}_{\mathcal{W}_k}^k - \mathbf{d}_N^k) = m_k(\mathbf{d}_{\mathcal{W}_k}^k) \leq m_k(\mathbf{0}) = 0$  due to the imposed conditions (10) (see Line 18 of Algorithm 1). We have for any  $\mathbf{d} \in \text{Lev}_{\bar{m}_k}$  that

$$\bar{\lambda}_{\min} \|\mathbf{d}\|^2 \leq \langle \mathbf{d}, \mathbf{H}^k \mathbf{d} \rangle \leq -\langle \mathbf{g}^k, \mathbf{d}_N^k \rangle,$$

where the second inequality holds by the definition of  $\text{Lev}_{\bar{m}_k}$  and makes use of (34). Therefore, we have

$$\|\mathbf{d}\|^2 \leq \frac{-\langle \mathbf{g}^k, \mathbf{d}_N^k \rangle}{\bar{\lambda}_{\min}}.$$

This, together with (35), (36) and the definition of  $\mathbf{d}_N^k$ , gives

$$\|\mathbf{d}_{\mathcal{W}_k}^k - \mathbf{d}_N^k\|^2 \leq \frac{-\langle \mathbf{g}^k, \mathbf{d}_N^k \rangle}{\bar{\lambda}_{\min}} \leq \frac{\|(\mathbf{H}^k)^{-1}\| \|\mathbf{g}^k\|^2}{\bar{\lambda}_{\min}} = \frac{\|\mathbf{g}^k\|^2}{(\bar{\lambda}_{\min})^2}. \quad (37)$$

Combining (37) with the triangle inequality and (35), we obtain

$$\|\mathbf{d}_{\mathcal{W}_k}^k\| \leq \|\mathbf{d}_{\mathcal{W}_k}^k - \mathbf{d}_N^k\| + \|\mathbf{d}_N^k\| \leq \frac{\|\mathbf{g}^k\|}{\lambda_{\min}} + \frac{\|\mathbf{g}^k\|}{\lambda_{\min}} = \frac{2\|\mathbf{g}^k\|}{\lambda_{\min}}.$$

In addition,  $\|\mathbf{d}_{\mathcal{W}_k}^k\| \geq \frac{\|\mathbf{g}^k\|}{\lambda_{\max}}$  is straightforwardly by (32). This completes the proof.  $\square$

## 2.4 Projected Line-search (Algorithm 3)

Once a descent direction  $\mathbf{d}$  is obtained by inexactly solving (29), SOIR $\ell_1$  implements a projected line-search [36] to determine a stepsize that ensures a sufficient decrease in  $F(\mathbf{x}; \epsilon)$ , as presented in Algorithm 3. We shall interpret Algorithm 3 line-by-line, omitting the iteration counter superscript  $k$  used in Algorithm 1.

Algorithm 3 consists of three main blocks. The first block corresponds to Lines 1–8. Starting with  $\mathbf{y}^j$  at the  $j$ th iteration. If  $\text{sgn}(\mathbf{y}^j) \neq \text{sgn}(\mathbf{x})$  holds, a line-search with backtracking is performed along direction  $\mathbf{d}$  to determine a stepsize  $\mu_j$  such that the projection  $\text{Proj}(\mathbf{x} + \mu_j \mathbf{d}; \mathbf{x})$  causes a decrease in  $F(\mathbf{x}; \epsilon)$ . If such a stepsize is found (i.e., Line 3 holds), it is deemed a “successful” step with no deterioration in the objective value and reduced support size. The line-search then terminates with  $\mathbf{y}^j \leftarrow \text{Proj}(\mathbf{x} + \mu_j \mathbf{d}; \mathbf{x})$ . Otherwise,  $\text{Proj}(\mathbf{x} + \mu_j \mathbf{d}; \mathbf{x})$  should have the same sign with  $\mathbf{x}$  after finite line-search trials. In this case, the first block terminates with  $j > 0$  and proceeds to the second block (see Lines 9–15).

Failure of the line-search with backtracking in the first block indicates that finding an iterate with an improved objective value and reduced support size compared to  $\mathbf{x}^k$  is unlikely. The algorithm then verifies a stepsize  $\mu_B = \arg \sup \{\mu > 0 : \text{sgn}(\mathbf{x} + \mu \mathbf{d}) = \text{sgn}(\mathbf{x})\}$ , which aims to yield a new iterate with reduced support (Lines 10). If  $\mathbf{x} + \mu_B \mathbf{d}$  causes a sufficient decrease in  $F(\mathbf{x}; \epsilon)$ , it is also deemed a “successful” stepsize (Line 14).

The definition of  $\mu_B$  implies that  $\mu_B$  is no less than the  $\mu_j$  found in the first block. Therefore, if  $\mu_B$  is successful, the algorithm will not proceed to the third block (Lines 16–22). If not, the loop in the third block continues the line-search with backtracking, terminating in a finite number of iterations.

Overall, we can conclude that  $\mathcal{I}(\mathbf{y}^j) = \mathcal{I}(\mathbf{x})$  if the Algorithm 3 is terminated in Line 18 and  $\mathcal{I}(\mathbf{y}^j) \subset \mathcal{I}(\mathbf{x})$  otherwise. The following lemma summarizes these interpretations of Algorithm 3.

**Lemma 5.** *Consider Algorithm 3. Let  $\mathbf{x}, \mathbf{d} \in \mathbb{R}^n$ ,  $\epsilon \in \mathbb{R}_+^n$  and  $\mathcal{W} \subseteq \mathcal{I}(\mathbf{x})$  such that  $\langle \nabla_{\mathcal{W}} F(\mathbf{x}; \epsilon), \mathbf{d}_{\mathcal{W}} \rangle < 0$  and  $\mathbf{d}_{\mathcal{W}^c} = \mathbf{0}$ . Then Algorithm 3 terminates finitely at some iteration number  $j_0$  and generates a value  $\mu_{j_0}$ . Moreover, if  $\text{sgn}(\mathbf{y}^{j_0}) \neq \text{sgn}(\mathbf{x})$ , we have*

$$\mu_{j_0} \geq \min(1, \mu_B) \quad \text{and} \quad |\mathcal{I}(\mathbf{y}^{j_0})| < |\mathcal{I}(\mathbf{x})|. \quad (38)$$

Otherwise,

$$\mu_{j_0} \geq \frac{2\xi(\varpi - 1) \langle \nabla_{\mathcal{W}} F(\mathbf{x}; \epsilon), \mathbf{d}_{\mathcal{W}} \rangle}{L_2(\mathbf{x}) \|\mathbf{d}_{\mathcal{W}}\|^2} \quad \text{and} \quad |\mathcal{I}(\mathbf{y}^{j_0})| = |\mathcal{I}(\mathbf{x})|, \quad (39)$$

---

**Algorithm 3** Projected line-search:  $[\mathbf{y}^j, \mu_j] := \text{PLS}(\mathbf{x}; \boldsymbol{\epsilon}, \mathbf{d}, \mathcal{W}; \varpi, \xi)$ 


---

**Require:**  $\{\mathbf{x}, \mathbf{d}, \boldsymbol{\epsilon}\} \in \mathbb{R}^n$ ,  $\mathcal{W} \subseteq \mathcal{I}(\mathbf{x})$ ;  $\varpi \in (0, \frac{1}{2})$  and  $\xi \in (0, 1)$ .

- 1: Set  $j \leftarrow 0$ ,  $\mu_0 \leftarrow 1$  and  $\mathbf{y}^0 \leftarrow \mathbb{P}(\mathbf{x} + \mathbf{d}; \mathbf{x})$ .
- 2: **while**  $\text{sgn}(\mathbf{y}^j) \neq \text{sgn}(\mathbf{x})$  **do**
- 3:   **if**  $F(\mathbf{y}^j; \boldsymbol{\epsilon}) \leq F(\mathbf{x}; \boldsymbol{\epsilon})$  **then**
- 4:     **return**  $\mathbf{y}^j$ .
- 5:   **end if**
- 6:   Set  $j \leftarrow j + 1$  and  $\mu_j = \xi \mu_{j-1}$ .
- 7:   Set  $\mathbf{y}^j \leftarrow \mathbb{P}(\mathbf{x} + \mu_j \mathbf{d}; \mathbf{x})$ .
- 8: **end while**
- 9: **if**  $j \neq 0$  **then**
- 10:   Set  $\mu_B \leftarrow \arg \sup \{\mu > 0 : \text{sgn}(\mathbf{x} + \mu \mathbf{d}) = \text{sgn}(\mathbf{x})\}$ .
- 11:   Set  $\mathbf{y}^j \leftarrow \mathbf{x} + \mu_B \mathbf{d}$ .
- 12:   **if**  $F(\mathbf{y}^j; \boldsymbol{\epsilon}) \leq F(\mathbf{x}; \boldsymbol{\epsilon}) + \varpi \mu_B \langle \nabla_{\mathcal{W}} F(\mathbf{x}; \boldsymbol{\epsilon}), \mathbf{d}_{\mathcal{W}} \rangle$  **then**
- 13:     **return**  $\mathbf{y}^j$ .
- 14:   **end if**
- 15: **end if**
- 16: **loop**
- 17:   **if**  $F(\mathbf{y}^j; \boldsymbol{\epsilon}) \leq F(\mathbf{x}; \boldsymbol{\epsilon}) + \varpi \mu_j \langle \nabla_{\mathcal{W}} F(\mathbf{x}; \boldsymbol{\epsilon}), \mathbf{d}_{\mathcal{W}} \rangle$  **then**
- 18:     **return**  $\mathbf{y}^j$ .
- 19:   **end if**
- 20:   Set  $j \leftarrow j + 1$  and  $\mu_j = \xi \mu_{j-1}$ .
- 21:   Set  $\mathbf{y}^j \leftarrow \mathbf{x} + \mu_j \mathbf{d}$ .
- 22: **end loop**

---

where  $F(\mathbf{x}; \boldsymbol{\epsilon})$  in the neighborhood  $\mathcal{B}(\mathbf{x}, \xi \mu_B \|\mathbf{d}\|)$  of  $\mathbf{x} \in \mathbb{R}^{|\mathcal{W}|}$  is Lipschitz differentiable with constant  $L_2(\mathbf{x}) > 0$  and  $\xi \in (0, 1)$ .

*Proof.* It suffices to restrict the discussion to the reduced space  $\mathbb{R}^{|\mathcal{W}|}$  since  $\mathbf{d}_{\mathcal{W}^c} = \mathbf{0}$ . Since  $\mathbf{x}_{\mathcal{W}}, \mathcal{W} \subseteq \mathcal{I}(\mathbf{x})$  is strictly in the interior of the “subspace orthant”  $\{\mathbf{z}_{\mathcal{W}} \in \mathbb{R}^{|\mathcal{W}|} \mid \text{sgn}(\mathbf{z}_{\mathcal{W}}) = \text{sgn}(\mathbf{x}_{\mathcal{W}})\} \neq \emptyset$ ,  $F(\mathbf{x}; \boldsymbol{\epsilon})$  is smooth in the subspace orthant around  $\mathbf{x}_{\mathcal{W}}$ . Hence, we can remove the subscript  $\mathcal{W}$  for brevity.

If  $\text{sgn}(\mathbf{y}^{j_0}) \neq \text{sgn}(\mathbf{x})$ , then Algorithm 3 terminates by Line 4 or Line 13. Therefore,  $F(\mathbf{y}^{j_0}; \boldsymbol{\epsilon}) \leq F(\mathbf{x}; \boldsymbol{\epsilon})$  naturally holds and  $\mathbf{y}^{j_0}$  is on the boundary of subspace orthant containing  $\mathbf{x}$  by (3), which means  $|\mathcal{I}(\mathbf{y}^{j_0})| < |\mathcal{I}(\mathbf{x})|$ .

If  $\text{sgn}(\mathbf{y}^{j_0}) = \text{sgn}(\mathbf{x})$ , then Algorithm 3 executes Line 16–22 and terminates by Line 18. When Line 16 is reached, there are two cases to consider.

- If  $j = 0$ , then  $\mathbf{x} + \mathbf{d}$  and  $\mathbf{x}$  are contained in the same orthant. In this case, there are no points of nondifferentiability of  $F(\mathbf{x}; \boldsymbol{\epsilon})$  exist on the line segment connecting  $\mathbf{x}$  to  $\mathbf{x} + \mathbf{d}$ . This also means  $\mu_0 = 1$  when reaching Line 18. The line-search with backtracking terminates at  $\mathbf{y}^0$ .
- If  $j > 0$ , then Line 10–14 are executed but the condition in Line 12 is violated.

Notice that  $\mathbf{x} + \mu_B \mathbf{d}$  is on the boundary of the orthant containing  $\mathbf{x}$  and there is also no points of nondifferentiability of  $F(\mathbf{x}; \boldsymbol{\epsilon})$  exist on the line segment connecting  $\mathbf{x}$  to  $\mathbf{x} + \mu_B \mathbf{d}$ . This also means  $\mu_j \geq \xi \mu_B$  when reaching Line 16.

In both cases, we end up with a traditional backtracking line-search with  $F(\mathbf{x}; \boldsymbol{\epsilon})$  being  $L_2(\mathbf{x})$ -Lipschitz differentiable in a neighborhood of  $\mathbf{x}$  (e.g., a ball centered at  $\mathbf{x}$  with radius  $\xi \alpha_B \|\mathbf{d}\|$ :  $\mathcal{B}(\mathbf{x}, \xi \mu_B \|\mathbf{d}\|)$ ). Now applying Taylor's Theorem,

$$F(\mathbf{x} + \mu \mathbf{d}; \boldsymbol{\epsilon}) - F(\mathbf{x}; \boldsymbol{\epsilon}) \leq \mu \langle \nabla F(\mathbf{x}; \boldsymbol{\epsilon}), \mathbf{d} \rangle + \frac{1}{2} \mu^2 L_2(\mathbf{x}) \|\mathbf{d}\|^2 \leq \varpi \mu \langle \nabla F(\mathbf{x}), \mathbf{d} \rangle,$$

where the second inequality is satisfied for any  $\mu \in \left(0, \frac{2(\varpi-1)\langle \nabla F(\mathbf{x}; \boldsymbol{\epsilon}), \mathbf{d} \rangle}{L_2(\mathbf{x}) \|\mathbf{d}\|^2}\right]$ . Therefore, the line-search with backtracking terminates with  $\mu$  that satisfies (39). The proof is complete.  $\square$

Overall, we have shown that SOIR $\ell_1$  is well-posed in the sense that each quadratic subproblem is well-defined (see Lemma 4), and the line-search procedures terminate in a finite number of iterations (see Lemma 2 and Lemma 5). We summarize these arguments in the following theorem.

**Theorem 5** (Well-posedness of SOIR $\ell_1$ ). *Suppose  $\tau = 0$ . Then Algorithm 1 will produce an infinite sequence  $\{(\mathbf{x}^k, \boldsymbol{\epsilon}^k)\}$ . Moreover, we have*

- (i)  $\{F(\mathbf{x}^k, \boldsymbol{\epsilon}^k)\}$  and  $\{\epsilon_i^k, i \in \mathcal{I}(\mathbf{x}^k)\}$  which are both monotonically nonincreasing and convergent.
- (ii)  $\{\mathbf{x}^k\} \subset \text{Lev}_F := \{\mathbf{x} \in \mathbb{R}^n \mid F(\mathbf{x}; \boldsymbol{\epsilon}) \leq F(\mathbf{x}^0; \boldsymbol{\epsilon}^0)\}$  and is bounded.

*Proof.* (i). Consider an arbitrary  $k \in \mathbb{N}$ . If  $\mathbf{x}^k$  are returned by IST step (see Lines 11, 14 and 22 of Algorithm 1), we then have from (22) and  $\boldsymbol{\epsilon}^{k+1} \leq \boldsymbol{\epsilon}^k$  (see Line 25 of Algorithm 1) that

$$F(\mathbf{x}^{k+1}; \boldsymbol{\epsilon}^{k+1}) \leq F(\mathbf{x}^k; \boldsymbol{\epsilon}^k) - \frac{\alpha}{2} \|\mathbf{x}^{k+1} - \mathbf{x}^k\|^2. \quad (40)$$

If  $\mathbf{x}^k$  are returned by Line 20 of Algorihtm 1, we have from Lemma 4 and Lemma 5 that  $F(\mathbf{x}^{k+1}; \boldsymbol{\epsilon}^{k+1}) \leq F(\mathbf{x}^k; \boldsymbol{\epsilon}^k)$ . This, together with (40), shows that  $\{F(\mathbf{x}^k; \boldsymbol{\epsilon}^k)\}$  is nonincreasing. Moreover, it follows from Assumption 1(i) that  $\{F(\mathbf{x}^k; \boldsymbol{\epsilon}^k)\}$  converges. By Algorithm 1, we see from Line 25 that  $\lim_{k \rightarrow +\infty} \epsilon_i^k = 0, i \in \mathcal{I}^k$ .

(ii). It follows from statement (i) that  $\mathbf{x}^k \subset \text{Lev}_F$ . On the other hand, by Assumption 1(i), we know that the level set  $\text{Lev}_F := \{\mathbf{x} \in \mathbb{R}^n : F(\mathbf{x}, \boldsymbol{\epsilon}) \leq F(\mathbf{x}^0, \boldsymbol{\epsilon}^0)\}$  is compact by noting that  $F$  is continuous and coercive. Hence,  $\{\mathbf{x}^k\}$  is bounded, as desired.  $\square$

**Remark 4.** *By the compactness of  $\text{Lev}_F$  and Theorem 5,  $f$  is Lipschitz differentiable over  $\text{Lev}_F$  with the Lipschitz constant  $L_f > 0$ . Additionally, there exists a constant  $\tilde{L}_f > 0$  such that  $\|\nabla^2 f(\mathbf{x})\| \leq \tilde{L}_f$  for any  $\mathbf{x} \in \text{Lev}_F$ . Hence, the local Lipschitz constant  $L_1(\mathbf{x})$  of  $f$ , as discussed in Lemma 2, satisfies  $L_1(\mathbf{x}) \leq L_f$  and can therefore be replaced by  $L_f$ . Regarding the Lipschitz constant  $L_2(\mathbf{x})$  of  $F(\mathbf{x}; \boldsymbol{\epsilon})$  restricted to the subspace in Lemma 5, it is also uniformly bounded above if the nonzero elements in*

all the iterates are uniformly bounded away from 0. This property is further analyzed in the subsequent section.

### 3 Convergence Analysis

In this section, we present the convergence analysis of the proposed SOIR $\ell_1$ . In the following, we set the tolerance  $\tau = 0$  and hence SOIR $\ell_1$  generates an infinite sequence  $\{\mathbf{x}^k\}_{k \in \mathbb{N}}$ . We first prove that the iterates generated by SOIR $\ell_1$  possess the locally stable support property after some finite iteration, which means that  $\mathcal{I}^k$  and  $\mathcal{I}_0^k$  remain unchanged after some  $k \in \mathbb{N}$ .

**Proposition 6** (Locally stable support). *Let  $\{\mathbf{x}^k\}$  be the sequence generated by Algorithm 1. The following statements hold.*

- (i) *There exists  $\delta > 0$  such that  $|x_i^k| > \delta, i \in \mathcal{I}^k$  holds true for all  $k$ . Consequently,  $\omega_i^k < \hat{\omega} := \lambda p \delta^{p-1}, i \in \mathcal{I}^k$  holds true for all  $k$ .*
- (ii) *There exist index sets  $\mathcal{I}_0^*$  and  $\mathcal{I}^*$  such that  $\mathcal{I}_0^k \equiv \mathcal{I}^*$  and  $\mathcal{I}^k \equiv \mathcal{I}^*$  for sufficiently large  $k$ .*
- (iii) *For any cluster point  $\mathbf{x}^*$  of  $\{\mathbf{x}^k\}$ ,  $\mathcal{I}_0(\mathbf{x}^*) = \mathcal{I}_0^*$  and  $\mathcal{I}(\mathbf{x}^*) = \mathcal{I}^*$ .*

*Proof.* (i) Suppose by contradiction that this is not true. Then there exist subsequence  $\mathcal{S} \in \mathbb{N}$  and an index  $j \in \mathcal{I}(\mathbf{x}^k)$  such that

$$|\mathcal{S}| = +\infty, \quad \{|x_j^k|\} \subset \mathbb{R}_{++} \quad \text{and} \quad \{|x_j^k|\}_{k \in \mathcal{S}} \rightarrow 0, \quad (41)$$

meaning  $\lim_{\mathcal{S} \ni k \rightarrow +\infty} \omega_j^k = +\infty$  and  $\lim_{k \rightarrow +\infty} \epsilon_j^k = 0$ .

We first show that  $x_j^{k+1} = 0$  for all sufficiently large  $k \in \mathcal{S}$ . Notice that index  $j$  is chosen by Line 13 in Algorithm 1 infinitely many times. If this were not the case,  $x_j^k$  would remain a positive constant for sufficiently large  $k$ , which would contradict (41).

Suppose now  $j$  is selected by Line 13 for sufficiently large  $k \in \mathcal{S}$  such that

$$\mu_{k+1} \omega_j^k \geq \min\{\bar{\mu}, \frac{\xi}{L_f + \alpha}\} \omega_j^k > R + \max\{\bar{\mu}, 1\} L_f \geq |x_j^k - \mu^{k+1} \nabla_j f(\mathbf{x}^k)|. \quad (42)$$

The first inequality of (42) is achieved by (21), and the second inequality is achieved by the argument  $\lim_{\substack{k \rightarrow +\infty \\ k \in \mathcal{S}}} \omega_j^k = +\infty$ , and the third inequality is achieved  $\{\nabla_j f(\mathbf{x}^k)\}$

and  $\{x_j^k\}$  are all bounded over  $\text{Lev}_F$  due to the same arguments presented in Lemma 4 indicated by Assumption 1(i). Here,  $R > 0$  refers to the radius of  $\mathcal{B}(0, R) = \{\mathbf{x} \in \mathbb{R}^n : \|\mathbf{x}\| \leq R\}$  containing  $\text{Lev}_F$ . The last inequality of (42) is achieved by the triangle inequality.

By Lemma A, we know that  $d_i(\mu_{k+1}) = -x_j^k$ . In other words, Line 14 returns  $\hat{\mathbf{x}}^{k+1}$  with  $\hat{x}_j^{k+1} = 0$ . This means  $\text{sgn}(\hat{\mathbf{x}}^{k+1}) \neq \text{sgn}(\mathbf{x}^k)$ , so that the QP subproblem is not triggered and  $\mathbf{x}^{k+1} = \hat{\mathbf{x}}^{k+1}$ .

Now  $j \in \mathcal{I}_0^{k+1}$ . We next show that  $j \in \mathcal{I}_0^k$  for  $\{k+1, k+2, \dots\}$  and  $k \in \mathcal{S}$ . This is true since the component  $x_j, j \in \mathcal{I}_0^k$  can only be changed if it is selected by the Line 10 at some  $\tilde{k} > k$ . However,  $\omega_j^{\tilde{k}} > \omega_j^k$  since  $x_j^k \neq 0$ ,  $x_j^{\tilde{k}} = 0$  and  $\epsilon_j^{\tilde{k}} = \epsilon_j^{k+1}$ , meaning

$\omega_j^{\tilde{k}} > L_f > |\nabla_j f(\mathbf{x}^k)|$  holds true by (42). This means  $j$  is never selected by (14) and Line 10, and will remain in  $\mathcal{I}_0^{\tilde{k}}$  for any  $\{k+1, k+2, \dots\}$ —contradicting (41).

(ii) Suppose by contradiction that this is not true. Then there exists  $j$  and  $\mathbb{N} = \mathcal{S} \cup \mathcal{S}_0$  such that  $|\mathcal{S}| = +\infty, |\mathcal{S}_0| = +\infty, x_j^k \in \mathcal{I}^k, k \in \mathcal{S}$  and  $x_j^k \in \mathcal{I}_0^k, k \in \mathcal{S}_0$ . It then follows from the update strategy of  $\epsilon$  (Lines 6 and 25) that  $\epsilon_j^k$  is reduced for all  $k \in \mathcal{S}$  and therefore  $\epsilon_j^k \rightarrow 0$ . Now for sufficiently large  $k \in \mathcal{S}_0$  satisfying  $\omega_j^k > L_f$  and  $[\Psi(\mathbf{x}^k, \epsilon^k)]_j = 0$ . Therefore,  $j$  will never be chosen by the Line 10 and will stay in  $\mathcal{I}_0^k$  for  $\{k+1, k+2, \dots\}$ , which means  $|\mathcal{S}| < +\infty$ —a contradiction.

(iii) Obvious. The proof is complete.  $\square$

### 3.1 Global convergence

The global convergence of SOIR $\ell_1$  is established in this subsection. For ease of presentation, we first define the following sets of iterations for our analysis.

$$\begin{aligned}\mathcal{S}_\Psi &:= \{k : \mathbf{x}^{k+1} \text{ is obtained from Line 11 at the } k\text{th iteration}\}, \\ \mathcal{S}_\Phi &:= \{k : \mathbf{x}^{k+1} \text{ is obtained from Line 22 at the } k\text{th iteration}\}, \\ \mathcal{S}_{QP} &:= \{k : \mathbf{x}^{k+1} \text{ is obtained from Line 20 at the } k\text{th iteration}\}.\end{aligned}$$

The set  $\mathcal{S}_\Psi$  includes iterations in which an IST subproblem is solved for the current zero components. The set  $\mathcal{S}_\Phi$  includes the iterations where an IST subproblem for the current nonzeros is solved. The set  $\mathcal{S}_{QP}$  includes the iterations in which the QP subproblem for current non-zeros is solved. We further spit  $\mathcal{S}_{QP}$  into two subsets based on whether the iterate returned by Algorithm 3 retains the same sign as  $\mathbf{x}^k$ .

$$\begin{aligned}\mathcal{S}_{QP}^N &:= \{k \in \mathcal{S}_{QP} : \text{sgn}(\mathbf{x}^{k+1}) \neq \text{sgn}(\mathbf{x}^k)\}, \\ \mathcal{S}_{QP}^Y &:= \{k \in \mathcal{S}_{QP} : \text{sgn}(\mathbf{x}^{k+1}) = \text{sgn}(\mathbf{x}^k)\}.\end{aligned}$$

By Lemma 5,  $k \in \mathcal{S}_{QP}^N$  means  $\mathbf{x}^{k+1}$  is updated by Algorithm 3 (Lines 1–8 or Line 9–15), while  $k \in \mathcal{S}_{QP}^Y$  means  $\mathbf{x}^{k+1}$  is updated by Algorithm 3 (Lines 16–22).

To show that our algorithm automatically reverts to a second-order method, we first show that the IST update (Lines 9–11) is never triggered for sufficiently large  $k$ .

**Theorem 7.** *The index sets  $|\mathcal{S}_\Psi| < +\infty, |\mathcal{S}_\Phi| < +\infty$  and  $|\mathcal{S}_{QP}^N| < +\infty$ .*

*Proof.* If Lines 9–11 are executed, then  $|\mathcal{I}^k| < |\mathcal{I}^{k+1}|$  by Lemma 3(i). However, this never happens for sufficiently large  $k$  by Proposition 6. Therefore,  $|\mathcal{S}_\Psi| < +\infty$ .

Suppose by contradiction that  $|\mathcal{S}_\Phi| = +\infty$ . It follows from (40) that for  $k \in \mathcal{S}_\Phi$

$$\begin{aligned}\sum_{k=0}^t [F(\mathbf{x}^k; \epsilon^k) - F(\mathbf{x}^{k+1}; \epsilon^{k+1})] &\geq \sum_{k \in \mathcal{S}_\Phi, k \leq t} [F(\mathbf{x}^k; \epsilon^k) - F(\mathbf{x}^{k+1}; \epsilon^{k+1})] \\ &\geq \frac{\alpha}{2} \sum_{k \in \mathcal{S}_\Phi, k \leq t} \|\mathbf{x}^k - \mathbf{x}^{k+1}\|^2.\end{aligned}$$

Letting  $t \rightarrow \infty$ , we obtain  $\mathbf{d}^k = \mathbf{x}^{k+1} - \mathbf{x}^k \rightarrow \mathbf{0}$ ,  $k \in \mathcal{S}_\Phi$ . There exists  $j \in \mathcal{I}^k$  such that  $\text{sgn}(\hat{x}_j^{k+1}) = \text{sgn}(x_j^k + \mu_k d_j^k) \neq \text{sgn}(x_j^k)$ ,  $k \in \mathcal{S}_\Phi$  by definition. However, by Proposition 6(i), for sufficiently large  $k \in \mathcal{S}_\Phi$ ,  $|\hat{x}_j^k| > \delta \geq 0$ . Therefore,  $\text{sgn}(x_j^k + \mu_k d_j^k) = \text{sgn}(x_j^k)$  for  $|d_j^k| < \frac{\delta}{2\bar{\mu}}$ , a contradiction. Hence,  $|\mathcal{S}_\Phi| < +\infty$ .

Suppose by contradiction that  $|\mathcal{S}_{\text{QP}}^N| = +\infty$ . By (38),  $\mathcal{I}(\mathbf{x}^{k+1}) \neq \mathcal{I}(\mathbf{x}^k)$  happens for infinitely many times, contradicting Proposition 6(ii). The proof is complete.  $\square$

We are now ready to prove the global convergence of the proposed algorithm.

**Theorem 8** (Global convergence of the whole iterates). *Let  $\{(\mathbf{x}^k, \boldsymbol{\epsilon}^k)\}_{k \in \mathbb{N}}$  be the sequence generated by Algorithm 1 and let  $(\mathbf{x}^*, \boldsymbol{\epsilon}^*)$  be the cluster point of  $\{(\mathbf{x}^k, \boldsymbol{\epsilon}^k)\}_{k \in \mathbb{N}}$ . It holds that*

$$\lim_{k \rightarrow +\infty} \Phi(\mathbf{x}^k, \boldsymbol{\epsilon}^k) = 0, \quad \lim_{k \rightarrow +\infty} \Psi(\mathbf{x}^k, \boldsymbol{\epsilon}^k) = 0, \quad \text{and} \quad \lim_{k \rightarrow +\infty} \epsilon_i^k = 0, \quad i \in \mathcal{I}^k.$$

Consequently,  $(\mathbf{x}^*, \boldsymbol{\epsilon}^*)$  is first-order stationary to  $(\mathcal{P})$ . Moreover, there exists a  $\hat{k}$  such that  $\epsilon_i^k \equiv \epsilon_i^{\hat{k}} > 0$ ,  $i \in \mathcal{I}_0^k$  for all  $k \geq \hat{k}$ . Therefore,  $\lim_{k \rightarrow +\infty} \boldsymbol{\epsilon}^k \rightarrow \boldsymbol{\epsilon}^*$  where  $\boldsymbol{\epsilon}_{\mathcal{I}^*}^* = \mathbf{0}$  and  $\boldsymbol{\epsilon}_{\mathcal{I}_0^*}^* = \boldsymbol{\epsilon}_{\mathcal{I}^*}^{\hat{k}}$ .

*Proof.* By Theorem 7, there exists  $\hat{k}$  such that  $\{\hat{k}, \hat{k} + 1, \dots\} \subset \mathcal{S}_{\text{QP}}^Y$  and Line 17 is triggered for each  $k \geq \hat{k}$ . Therefore, it follows that

$$\begin{aligned} F(\mathbf{x}^k; \boldsymbol{\epsilon}^k) - F(\mathbf{x}^{k+1}; \boldsymbol{\epsilon}^k) &\geq -\varpi \mu_k \langle \nabla_{\mathcal{W}_k} F(\mathbf{x}^k; \boldsymbol{\epsilon}^k), \mathbf{d}_{\mathcal{W}_k}^k \rangle \\ &\geq \frac{2\varpi \xi (1-\varpi) |\langle \nabla_{\mathcal{W}_k} F(\mathbf{x}^k; \boldsymbol{\epsilon}^k), \mathbf{d}_{\mathcal{W}_k}^k \rangle|^2}{\bar{\lambda}_{\max} \|\mathbf{d}_{\mathcal{W}_k}^k\|^2} \geq \frac{\varpi \xi (1-\varpi) \bar{\lambda}_{\min}^2}{2\bar{\lambda}_{\max}^3} \|\nabla_{\mathcal{W}_k} F(\mathbf{x}^k; \boldsymbol{\epsilon}^k)\|^2, \end{aligned} \quad (43)$$

where  $\bar{\lambda}_{\max} \geq L_2(\mathbf{x}^k)$  and  $\bar{\lambda}_{\min}$  are defined in Assumption 4 since Proposition 6(i) holds. The second inequality holds by (39) and the last inequality holds by (30), (32) and (33). This, combined with (16), yields that for  $k \geq \hat{k}$ ,  $k \in \mathcal{S}_{\text{QP}}^Y$

$$\begin{aligned} F(\mathbf{x}^k; \boldsymbol{\epsilon}^k) - F(\mathbf{x}^{k+1}; \boldsymbol{\epsilon}^{k+1}) &\geq F(\mathbf{x}^k; \boldsymbol{\epsilon}^k) - F(\mathbf{x}^{k+1}; \boldsymbol{\epsilon}^k) \\ &\geq \frac{\varpi \xi (1-\varpi) \bar{\lambda}_{\min}^2}{2\bar{\lambda}_{\max}^3} \|[\Phi^k]_{\mathcal{W}_k}\|^2 \geq \frac{\eta_\Phi \varpi \xi (1-\varpi) \bar{\lambda}_{\min}^2}{2\bar{\lambda}_{\max}^3} \|[\Phi^k]_{\mathcal{I}^k}\|^2 \\ &= \frac{\eta_\Phi \varpi \xi (1-\varpi) \bar{\lambda}_{\min}^2}{2\bar{\lambda}_{\max}^3} \|\Phi^k\|^2, \end{aligned}$$

where the third inequality holds by Line 13 of Algorithm 1 and the equality holds by (15). Summing up both sides from  $\hat{k}$  to  $t$  and letting  $t \rightarrow \infty$ , we immediately have  $\|\Phi^k\| \rightarrow 0$  as  $k \rightarrow +\infty$ . On the other hand, since  $\{\hat{k}, \hat{k} + 1, \dots\} \subset \mathcal{S}_{\text{QP}}^Y$ ,  $\|\Psi^k\| < \gamma \|\Phi^k\|$  is satisfied for all  $k \geq \hat{k}$ . Then, we know that  $\|\Psi^k\| \rightarrow 0$  as  $k \rightarrow +\infty$ . Consequently, it follows Proposition 3(iii) that  $(\mathbf{x}^*, \boldsymbol{\epsilon}^*)$  is first-order stationary to  $(\mathcal{P})$ . Moreover, Theorem 6 implies that  $\epsilon_i^k \rightarrow 0$ ,  $i \in \mathcal{I}^k$  and  $\epsilon_i^k \equiv \epsilon_i^{\hat{k}} > 0$ ,  $i \in \mathcal{I}_0^k$  for all  $k \geq \hat{k}$ . The proof is complete.  $\square$

Theorem 8 implies that there exists  $\hat{k}$  such that for all  $k \geq \hat{k}$ ,  $(\mathbf{x}^k, \boldsymbol{\epsilon}^k)$  always stays in the reduced subspace

$$\mathcal{M}(\mathbf{x}^*, \boldsymbol{\epsilon}^*) := \{(\mathbf{x}, \boldsymbol{\epsilon}) \mid \mathbf{x}_{\mathcal{I}_0^*} = \mathbf{0}, \boldsymbol{\epsilon}_{\mathcal{I}_0^*} \equiv \boldsymbol{\epsilon}_{\mathcal{I}_0^*}^{\hat{k}}\},$$

and  $\mathbf{x}^k$  is contained in the reduced subspace  $\overline{\mathcal{M}}(\mathbf{x}^*) := \{\mathbf{x} \mid \mathbf{x}_{\mathcal{I}_0^*} = \mathbf{0}\}$ . The local equivalence between  $\Phi$  and the subspace gradient of  $F(\mathbf{x}; \boldsymbol{\epsilon})$  also follows from Theorem 8, as we shown in the following corollary.

**Corollary 1.** *Let  $\{(\mathbf{x}^k, \boldsymbol{\epsilon}^k)\}_{k \in \mathbb{N}}$  be the sequence generated by Algorithm 1. Then  $\Phi_i^k = \nabla_i F(\mathbf{x}^k; \boldsymbol{\epsilon}^k), i \in \mathcal{I}^*$  for sufficiently large  $k$ . Thus,  $\lim_{k \rightarrow +\infty} \nabla_{\mathcal{I}^*} F(\mathbf{x}^k; \boldsymbol{\epsilon}^k) = 0$ .*

*Proof.* It suffices to prove the second and third cases in (15). For  $i \in \mathcal{I}_+^k$  and  $\nabla_i f(\mathbf{x}^k) + \omega_i^k > 0$ , Theorem 6 implies that  $\max\{x_i^k, \nabla_i f(\mathbf{x}^k) - \omega_i^k\} > \delta > 0$ . Note that  $\Phi_i^k \rightarrow 0$  by Theorem 8. This implies that  $\Phi_i^k = \nabla_i f(\mathbf{x}^k) + \omega_i = \nabla_i F(\mathbf{x}^k; \boldsymbol{\epsilon}^k)$  for all sufficiently large  $k$ . For  $i \in \mathcal{I}_-^k$  and  $\nabla_i f(\mathbf{x}^k) - \omega_i^k < 0$ , similar arguments establishes  $\Phi_i^k = \nabla_i f(\mathbf{x}^k) + \omega_i = \nabla_i F(\mathbf{x}^k; \boldsymbol{\epsilon}^k)$  for all sufficiently large  $k$ . The proof is complete.  $\square$

### 3.2 Convergence rate under the Kurdyka-Łojasiewicz property

In this subsection, we establish the local convergence properties by leveraging the well-known KL property. For completeness, we first recall some essential elements of the KL property [38], including the KL inequality and KL exponent.

**Definition 2** (KL property & KL function). *The function  $F : \mathbb{R}^n \rightarrow \mathbb{R} \cup \{+\infty\}$  is said to satisfy the Kurdyka-Łojasiewicz property in  $\bar{\mathbf{x}} \in \text{dom} \bar{\partial}F = \{\mathbf{x} \in \mathbb{R}^n \mid \bar{\partial}F \neq \emptyset\}$  if there exist  $\varsigma \in (0, +\infty]$ , a neighborhood  $\mathcal{N}$  of  $\bar{\mathbf{x}}$  and a continuous concave function  $\varphi : [0, \varsigma) \rightarrow \mathbb{R}_+$  such that*

- (i)  $\varphi(0) = 0$ ;
- (ii)  $\varphi$  is  $C^1$  on  $(0, \varsigma)$  and continuous at 0;
- (iii)  $\varphi'(s) > 0$  for all  $s \in (0, \varsigma)$ ;
- (iv) the Kurdyka-Łojasiewicz inequality holds, i.e.,

$$\varphi'(F(\mathbf{x}) - F(\bar{\mathbf{x}})) \text{dist}(0, \bar{\partial}F(\mathbf{x})) \geq 1 \quad (\text{KL})$$

holds, for all  $\mathbf{x}$  in the strict local upper level set  $\text{Lev}_\varsigma(\bar{\mathbf{x}}) = \{\mathbf{x} \in \mathcal{N} \mid F(\bar{\mathbf{x}}) < F(\mathbf{x}) < F(\bar{\mathbf{x}}) + \varsigma\}$ .

A proper lower-semicontinuous function satisfying the KL property at any  $\mathbf{x} \in \mathbb{R}^n$  is said to be a KL function.

**Definition 3** (KL exponent [39, Definition 2.3]). *For a proper closed function  $F$  satisfying the KL property at  $\bar{\mathbf{x}} \in \text{dom} \bar{\partial}F$ , if the corresponding function  $\varphi$  takes the form of  $\varphi(s) = cs^{1-\theta}$  for some  $c > 0$  and  $\theta \in [0, 1)$ , i.e., there exist  $c, \rho > 0$  and  $\varsigma \in (0, +\infty]$  such that  $\text{dist}(0, \bar{\partial}F(\mathbf{x})) \geq c(F(\mathbf{x}) - F(\bar{\mathbf{x}}))^\theta$  whenever  $\|\mathbf{x} - \bar{\mathbf{x}}\| \leq \rho$  and  $F(\bar{\mathbf{x}}) < F(\mathbf{x}) < F(\bar{\mathbf{x}}) + \varsigma$ , then we say that  $F$  has the KL property at  $\bar{\mathbf{x}}$  with an exponent of  $\theta$ . If  $F$  is a KL function and has the same exponent  $\theta$  at any  $\bar{\mathbf{x}} \in \text{dom} \bar{\partial}F$ , then we say that  $F$  is a KL function with an exponent of  $\theta$ .*

Proposition 6 and Theorem 8 indicate that  $x_i^k \equiv 0$  and  $\epsilon_i^k \equiv \hat{\epsilon}_i^k, i \in \mathcal{I}_0^*$  for any  $k \geq \hat{k}$ , and the iterates  $\{x_{\mathcal{I}}^*\}_{k \geq \hat{k}}$  strictly remain in the interior of reduced subspace  $\mathbb{R}^{|\mathcal{I}^*|}$ . Therefore, we restrict our discussion to the formed subspace  $\mathbb{R}^{|\mathcal{I}^*|}$ . In addition, we denote  $\boldsymbol{\epsilon} = \boldsymbol{\epsilon} \circ \boldsymbol{\epsilon}$  by  $\boldsymbol{\epsilon} \geq \mathbf{0}$  and treat  $\boldsymbol{\epsilon}$  as a variable.

As noted in [40, Page 63, Section 2.1], determining or estimating the KL exponent of a given function is often extremely challenging. A particularly relevant and useful result is the following theorem provided in [41], with a thorough proof in [15, Theorem 7]. It claims that a smooth function has a KL exponent  $\theta = 1/2$  at a non-degenerate critical point, where the Hessian is non-singular. Based on this, we can derive the following result.

**Proposition 9.** *Consider the following four cases.*

- (i) *The KL exponent of  $F(\mathbf{x}, \boldsymbol{\epsilon})$  restricted on  $\mathcal{M}(\mathbf{x}^*, \boldsymbol{\epsilon}^*)$  at  $(\mathbf{x}_{\mathcal{I}^*}^*, \mathbf{0})$  is  $\theta$ .*
- (ii) *The KL exponent of  $F(\mathbf{x}, \boldsymbol{\epsilon})$  at  $(\mathbf{x}^*, \mathbf{0})$  is  $\theta$ .*
- (iii) *The KL exponent of  $F(\mathbf{x})$  restricted on  $\overline{\mathcal{M}}(\mathbf{x}^*)$  at  $\mathbf{x}_{\mathcal{I}^*}^*$  is  $\theta$ .*
- (iv) *The KL exponent of  $F(\mathbf{x})$  at  $\mathbf{x}^*$  is  $\theta$ .*

Then we have (i)  $\iff$  (ii), (iii)  $\iff$  (iv), and (i)  $\implies$  (iii). Moreover, we have  $\theta \in (0, 1)$  and  $\theta = 1/2$  if  $\nabla_{\mathcal{I}^*}^2 F(\mathbf{x}^*)$  is nonsingular in (iii).

*Proof.* Since  $F(\mathbf{x}, \boldsymbol{\epsilon})$  is restricted on  $\mathcal{M}(\mathbf{x}^*, \boldsymbol{\epsilon}^*)$ , there exists a sufficiently small  $\rho > 0$  such that  $F(\mathbf{x}, \boldsymbol{\epsilon})$  is differentiable with  $\nabla F$  strictly continuous on  $\mathcal{B}((\mathbf{x}_{\mathcal{I}^*}^*, \mathbf{0}), \rho)$ . By [42, Example 3.1] and [1, Proposition 13.14], we know that  $F$  is prox-regular [1, Definition 13.27] and  $\mathcal{C}^2$ -partly smooth [42, Definition 2.7] at  $(\mathbf{x}_{\mathcal{I}^*}^*, \mathbf{0})$ . In addition, we have from Theorem 8 that  $\mathbf{0} \in \text{ri} \partial F(\mathbf{x}_{\mathcal{I}^*}^*, \mathbf{0})$ . Therefore, it follows from [39, Theorem 3.7] that (i)  $\implies$  (ii).

Conversely, since  $F(\mathbf{x}, \boldsymbol{\epsilon})$  has the KL exponent  $\theta$  at  $(\mathbf{x}^*, \mathbf{0})$ , there exist  $\varsigma > 0$ ,  $\rho > 0$  and  $c > 0$  such that for all  $(\mathbf{x}^*, \mathbf{0}) \in \text{Lev}_\varsigma(\mathbf{x}^*, \mathbf{0})$  with  $\text{Lev}_\varsigma(\mathbf{x}^*, \mathbf{0}) = \{(\mathbf{x}, \boldsymbol{\epsilon}) \in \mathcal{B}((\mathbf{x}^*, \mathbf{0}), \rho) \mid F(\mathbf{x}^*, \mathbf{0}) < F(\mathbf{x}, \boldsymbol{\epsilon}) < F(\mathbf{x}^*, \mathbf{0}) + \varsigma\}$ ,

$$\text{dist}(0, \partial F(\mathbf{x}, \boldsymbol{\epsilon})) \geq c(F(\mathbf{x}, \boldsymbol{\epsilon}) - F(\mathbf{x}^*, \mathbf{0}))^\theta$$

Since  $x_i^* \neq 0$  for any  $i \in \mathcal{I}^*$ , there exists  $\hat{\rho} > 0$  such that for all  $(\mathbf{z}, \mathbf{0}) \in \mathcal{B}(\mathbf{x}_{\mathcal{I}^*}^*, \mathbf{0})$ ,  $z_i \neq 0, i \in \mathcal{I}^*$ . Let  $\tilde{\rho} = \min(\rho, \hat{\rho})$ . Consider any  $(\mathbf{x}, \boldsymbol{\epsilon}) \in \mathcal{M}(\mathbf{x}^*, \boldsymbol{\epsilon}^*)$ . It implies that  $(\mathbf{x}_{\mathcal{I}^*}, \boldsymbol{\epsilon}_{\mathcal{I}^*}) \in \text{Lev}_\varsigma(\mathbf{x}_{\mathcal{I}^*}^*, \mathbf{0})$  with  $\text{Lev}_\varsigma(\mathbf{x}_{\mathcal{I}^*}^*, \mathbf{0}) = \{(\mathbf{x}_{\mathcal{I}^*}, \boldsymbol{\epsilon}_{\mathcal{I}^*}) \in \mathcal{B}((\mathbf{x}_{\mathcal{I}^*}^*, \mathbf{0}), \tilde{\rho}) \mid F(\mathbf{x}_{\mathcal{I}^*}^*, \mathbf{0}) \leq F(\mathbf{x}_{\mathcal{I}^*}, \boldsymbol{\epsilon}_{\mathcal{I}^*}) \leq F(\mathbf{x}_{\mathcal{I}^*}^*, \mathbf{0}) + \varsigma\}$ . Hence, we know that

$$\begin{aligned} \|\nabla_{\mathcal{I}^*} F(\mathbf{x}^*, \mathbf{0})\| &= \text{dist}(0, \partial F(\mathbf{x}, \boldsymbol{\epsilon})) \geq c(F(\mathbf{x}, \boldsymbol{\epsilon}) - F(\mathbf{x}^*, \mathbf{0}))^\theta \\ &= c(F(\mathbf{x}_{\mathcal{I}^*}, \boldsymbol{\epsilon}_{\mathcal{I}^*}) - F(\mathbf{x}_{\mathcal{I}^*}^*, \mathbf{0}))^\theta. \end{aligned} \tag{44}$$

This completes the proof of conclusion (i)  $\iff$  (ii). The proof of (iii)  $\iff$  (iv) can be finished using similar arguments by setting  $\boldsymbol{\epsilon} \equiv \mathbf{0}$ .

We now prove (i)  $\implies$  (iii). Note that  $\varepsilon_{\mathcal{I}^*}^* = \mathbf{0}$  and  $\frac{\partial}{\partial \varepsilon_{\mathcal{I}^*}} F(\mathbf{x}^*, \varepsilon^*) = 2\omega_{\mathcal{I}^*}^* \circ \varepsilon_{\mathcal{I}^*}^* = \mathbf{0}$ . By Definition 3 and (i), there exists  $c > 0$ , such that

$$\begin{aligned} \|\nabla_{\mathcal{I}^*} F(\mathbf{x})\| &= \left\| \begin{bmatrix} \frac{\partial}{\partial \mathbf{x}_{\mathcal{I}^*}} F(\mathbf{x}, \varepsilon^*) \\ 0 \end{bmatrix} \right\| = \|\nabla_{\mathcal{I}^*} F(\mathbf{x}, \varepsilon^*)\| \\ &\geq c(F(\mathbf{x}, \varepsilon^*) - F(\mathbf{x}^*, \varepsilon^*))^\theta \geq c(F(\mathbf{x}) - F(\mathbf{x}^*))^\theta \end{aligned}$$

indicating (iii) holds.

Moreover, if  $\nabla_{\mathcal{I}^*}^2 F(\mathbf{x}^*)$  is nonsingular, [15, Theorem 6] indicates that the KL exponent of (c) is  $1/2$ . In addition,  $\|\nabla_{\mathcal{I}^*} F(\mathbf{x})\| \geq c(F(\mathbf{x}) - F(\mathbf{x}^*))^\theta$  cannot be true, so that  $\theta \neq 0$ .  $\square$

The convergence rate analysis of IR $\ell_1$ -type methods for  $\ell_p$ -regularized problems ( $\mathcal{P}$ ) under the KL property has been studied in [14, 15]. For further insights into convergence rate analysis for a broader range of descent methods, we refer readers to [39, 43, 44].

We proceed to demonstrate that SOIR $\ell_1$  satisfies both the *sufficient decrease condition* and the *relative error condition* as outlined in [43–45]. From here, the analysis becomes straightforward and can be derived using standard arguments.

**Theorem 10.** *Let  $\{(\mathbf{x}^k, \varepsilon^k)\}$  be the sequence generated by Algorithm 1. Then the following statements hold.*

(i) *(sufficient decrease condition) There exists  $C_1 > 0$  such that*

$$F(\mathbf{x}^{k+1}, \varepsilon^{k+1}) + C_1 \|\mathbf{x}^{k+1} - \mathbf{x}^k\|^2 \leq F(\mathbf{x}^k, \varepsilon^k).$$

(ii) *(relative error condition) There exists  $C_2 > 0$  such that*

$$\|\nabla F(\mathbf{x}^{k+1}, \varepsilon^{k+1})\| \leq C_2 (\|\mathbf{x}^{k+1} - \mathbf{x}^k\| + \|\varepsilon^k\|_1 - \|\varepsilon^{k+1}\|_1).$$

Moreover, suppose that  $F(\mathbf{x}, \varepsilon)$  restricted to  $\mathcal{M}(\mathbf{x}^*, \varepsilon^*)$  is a KL function at all stationary points  $(\mathbf{x}^*, \mathbf{0})$  with  $\mathcal{I}(\mathbf{x}^*) = \mathcal{I}^*$  and  $\nabla_{\mathcal{I}^*} F(\mathbf{x}^*; \mathbf{0}) = \mathbf{0}$ . Then it holds that

(iii)  $\{\mathbf{x}^k\}$  converges to a stationary point  $\mathbf{x}^*$  and  $\sum_{k=0}^{+\infty} \|\mathbf{x}^{k+1} - \mathbf{x}^k\| < +\infty$ .

In addition, if  $\varphi(s) = cs^{1-\theta}$  for some  $\theta \in [0, 1)$  and  $c > 0$ . Then for sufficiently large  $k$  it holds that

(iv) If  $\theta \in (0, \frac{1}{2}]$ , then there exists  $\vartheta \in (0, 1)$ ,  $c_1 > 0$  such that  $\|\mathbf{x}^k - \mathbf{x}^*\| < c_1 \vartheta^k$ .

(v) If  $\theta \in (\frac{1}{2}, 1)$ , then there exist  $c_2 > 0$  such that  $\|\mathbf{x}^k - \mathbf{x}^*\| < c_2 k^{-\frac{1-\theta}{2\theta-1}}$ .

*Proof.* For brevity and without loss of generality, we remove the subscript  $\mathcal{I}^*$  in this proof. Write  $\nabla_{\mathbf{x}} F(\mathbf{x}, \varepsilon)$  for  $\frac{\partial}{\partial \mathbf{x}_{\mathcal{I}^*}} F(\mathbf{x}, \varepsilon)$  and  $\nabla_{\varepsilon} F(\mathbf{x}, \varepsilon)$  for  $\frac{\partial}{\partial \varepsilon_{\mathcal{I}^*}} F(\mathbf{x}, \varepsilon)$ .

(i). It follows from (43) that

$$\begin{aligned}
& F(\mathbf{x}^k; \boldsymbol{\epsilon}^k) - F(\mathbf{x}^{k+1}; \boldsymbol{\epsilon}^{k+1}) \\
& \geq \frac{\varpi \xi (1-\varpi) \bar{\lambda}_{\min}^2}{2 \bar{\lambda}_{\max}^3} \|\nabla F(\mathbf{x}^k; \boldsymbol{\epsilon}^k)\|^2 \geq \frac{\varpi \xi (1-\varpi) \bar{\lambda}_{\min}^2}{2 \bar{\lambda}_{\max}^3} \cdot \frac{\bar{\lambda}_{\min}^2}{4} \|\mathbf{d}^k\|^2 \\
& \geq C_1 := \frac{\varpi \xi (1-\varpi) \bar{\lambda}_{\min}^2}{2 \bar{\lambda}_{\max}^3} \cdot \frac{\bar{\lambda}_{\min}^2}{4} \|\mu_k \mathbf{d}^k\|^2 = C_1 \|\mathbf{x}^{k+1} - \mathbf{x}^k\|^2,
\end{aligned}$$

where the second inequality is by (33) and the last inequality holds since  $\mu_k \leq \mu_0 = 1$ .

(ii). We first establish an upper bound of  $\|\nabla_{\mathbf{x}} F(\mathbf{x}^{k+1}, \boldsymbol{\epsilon}^{k+1})\|$ .

$$\begin{aligned}
\|\nabla_{\mathbf{x}} F(\mathbf{x}^{k+1}, \boldsymbol{\epsilon}^{k+1})\| & \leq \|\nabla_{\mathbf{x}} F(\mathbf{x}^{k+1}, \boldsymbol{\epsilon}^{k+1}) - \nabla_{\mathbf{x}} F(\mathbf{x}^k, \boldsymbol{\epsilon}^k)\| + \|\nabla_{\mathbf{x}} F(\mathbf{x}^k, \boldsymbol{\epsilon}^k)\| \\
& \leq \|\nabla f(\mathbf{x}^{k+1}) - \nabla f(\mathbf{x}^k)\| + \|\boldsymbol{\omega}(\mathbf{x}^{k+1}, (\boldsymbol{\epsilon}^{k+1})^2) - \boldsymbol{\omega}(\mathbf{x}^k, (\boldsymbol{\epsilon}^k)^2)\| + \|\nabla_{\mathbf{x}} F(\mathbf{x}^k, \boldsymbol{\epsilon}^k)\|.
\end{aligned}$$

By the Lipschitz property of  $f$ , the first term is bounded by

$$\|\nabla f(\mathbf{x}^{k+1}) - \nabla f(\mathbf{x}^k)\| \leq L \|\mathbf{x}^{k+1} - \mathbf{x}^k\|.$$

Now we give an upper bound for the third term. Combining (39), (32) and (33), we have for  $k \geq \hat{k}$ ,

$$\begin{aligned}
\|\mathbf{x}^{k+1} - \mathbf{x}^k\| & = \|\mu_k \mathbf{d}^k\| \geq \frac{2\xi(1-\varpi)|\langle \mathbf{g}^k, \mathbf{d}^k \rangle|}{L_F \|\mathbf{d}^k\|^2} \frac{\|\mathbf{g}^k\|}{\bar{\lambda}_{\max}} \\
& \geq \frac{\xi(1-\varpi) \bar{\lambda}_{\min}^2}{2L_F \bar{\lambda}_{\max}^2} \|\nabla_{\mathbf{x}} F(\mathbf{x}^k, \boldsymbol{\epsilon}^k)\|.
\end{aligned}$$

Finally, we give an upper bound for the second term. From [14, Lemma 1], we have the change between  $\boldsymbol{\omega}^{k+1} := \boldsymbol{\omega}(\mathbf{x}^{k+1}, (\boldsymbol{\epsilon}^{k+1})^2)$  and  $\boldsymbol{\omega}^k := \boldsymbol{\omega}(\mathbf{x}^k, (\boldsymbol{\epsilon}^k)^2)$  is bounded by,

$$\|\boldsymbol{\omega}^{k+1} - \boldsymbol{\omega}^k\| \leq \bar{C}[\sqrt{|\mathcal{I}^*|} \|\mathbf{x}^{k+1} - \mathbf{x}^k\| + 2\|\boldsymbol{\epsilon}^0\|_{\infty}(\|\boldsymbol{\epsilon}^k\|_1 - \|\boldsymbol{\epsilon}^{k+1}\|_1)],$$

where  $\bar{C} := \lambda p(1-p)(\delta)^{p-2}$ . Putting together the bounds for all three terms, we have

$$\begin{aligned}
\|\nabla_{\mathbf{x}} F(\mathbf{x}^{k+1}, \boldsymbol{\epsilon}^{k+1})\| & \leq (L + \frac{2L_F \bar{\lambda}_{\max}^2}{\xi(1-\varpi) \bar{\lambda}_{\min}^2} + \bar{C} \sqrt{|\mathcal{I}^*|}) \|\mathbf{x}^{k+1} - \mathbf{x}^k\|_2 \\
& \quad + 2\|\boldsymbol{\epsilon}^0\|_{\infty} \bar{C}(\|\boldsymbol{\epsilon}^k\|_1 - \|\boldsymbol{\epsilon}^{k+1}\|_1).
\end{aligned} \tag{45}$$

On the other hand,

$$\begin{aligned}
\|\nabla_{\boldsymbol{\epsilon}} F(\mathbf{x}^{k+1}, \boldsymbol{\epsilon}^{k+1})\| & \leq \|\nabla_{\boldsymbol{\epsilon}} F(\mathbf{x}^{k+1}, \boldsymbol{\epsilon}^{k+1})\|_1 = \sum_{i \in \mathcal{I}^*} 2[\omega(\mathbf{x}^{k+1}, (\boldsymbol{\epsilon}^{k+1})^2)]_i \cdot \boldsymbol{\epsilon}_i^{k+1} \\
& \leq \sum_{i \in \mathcal{I}^*} 2\hat{\omega} \frac{\sqrt{\beta}}{1 - \sqrt{\beta}} (\boldsymbol{\epsilon}_i^k - \boldsymbol{\epsilon}_i^{k+1}) \leq 2\hat{\omega} \frac{\sqrt{\beta}}{1 - \sqrt{\beta}} (\|\boldsymbol{\epsilon}^k\|_1 - \|\boldsymbol{\epsilon}^{k+1}\|_1)
\end{aligned} \tag{46}$$

where the second inequality holds by 6 and  $\epsilon^{k+1} \leq \sqrt{\beta}\epsilon^k$ . Overall, we obtain from (45) and (46) that

$$\|\nabla F(\mathbf{x}^{k+1}, \epsilon^{k+1})\| \leq C_2(\|\mathbf{x}^{k+1} - \mathbf{x}^k\| + \|\epsilon^k\|_1 - \|\epsilon^{k+1}\|_1),$$

where

$$C_2 := \max\{L + \frac{2L_F \bar{\lambda}_{\max}^2}{\xi(1-\varpi)\bar{\lambda}_{\min}^2} + \bar{C}\sqrt{|\mathcal{I}^*|}, 2\|\epsilon^0\|_\infty \bar{C} + 2\hat{\omega} \frac{\sqrt{\beta}}{1-\sqrt{\beta}}\}.$$

(iii)(iv)(v) The three statements follow the standard analysis for perturbed functions with the KL property. Consequently, (iii) essentially follows from the convergence analysis of [43, Theorem 2.9] or [44, Theorem 4] and (iv),(v) can be derived using the same arguments as in the proofs of [14, Theorem 4] and [15, Theorem 4]. Therefore, the proof is omitted.  $\square$

### 3.3 Local convergence analysis with exact QP solution

In this subsection, we establish the local convergence properties of Algorithm 1 in the locally neighborhood of stationary points. By Proposition 6, after a finite number of iterations, the iterates generated by SOIR $\ell_1$  are obtained through solving only a reduced-space QP subproblem combined with a backtracking line-search. For the purpose of this analysis, let  $\chi^\infty$  be the set consisting of all stationary points of  $\{\mathbf{x}^k\}$  generated by SOIR $\ell_1$ , and we make the following assumptions.

**Assumption 11.** Suppose  $\{\mathbf{x}^k\}$  is generated by Algorithm 1 with  $\{\mathbf{x}^k\} \rightarrow \mathbf{x}^* \in \chi^\infty$ . For all sufficiently large  $k$ , we assume

- (i) The exact Hessian  $\mathbf{H}^k = \nabla_{\mathcal{I}^k \mathcal{I}^k}^2 F(\mathbf{x}^k; \epsilon^k)$  is used in  $m_k(\mathbf{d})$  and  $\mathcal{W}_k \equiv \mathcal{I}^k$ .
- (ii) The reduced-space QP subproblem (29) is solved exactly i.e.,  $\mathbf{d}_{\mathcal{W}_k}^k = (\mathbf{H}^k)^{-1} \mathbf{g}^k$ .
- (iii) For all sufficiently large  $k$ , unit stepsize  $\mu_k \equiv 1$  is accepted.
- (iv) There exists  $M > 0$  such that reduced-space Hessian of  $F(\mathbf{x})$  at  $\mathbf{x}^*$  satisfying  $\|\nabla_{\mathcal{I}^* \mathcal{I}^*}^2 F(\mathbf{x}^*)^{-1}\| \leq M$ .

As shown in Proposition 9, the non-singularity of  $\nabla_{\mathcal{I}^* \mathcal{I}^*}^2 F(\mathbf{x})$  implies the KL exponent of  $F$  is  $1/2$  at  $\mathbf{x}^*$ . Therefore, a linear convergence rate is achieved by Theorem 10. In the following, we show that under Assumption 11, a quadratic convergence rate can be attained when  $\epsilon_{\mathcal{I}^*}^k \rightarrow \mathbf{0}$  at a quadratic rate.

**Theorem 12.** Suppose Assumption 11 hold. Let  $\{(\mathbf{x}^k, \epsilon^k)\}$  be the sequence generated by Algorithm 1 and  $\{\mathbf{x}^k\} \rightarrow \mathbf{x}^* \in \chi^\infty$ . Then there exist  $\hat{k} \in \mathbb{N}$  and  $\rho > 0$  such that for all  $\mathbf{x}^k \in \mathcal{B}(\mathbf{x}^*, \rho)$  satisfies

$$\|\mathbf{x}^{k+1} - \mathbf{x}^*\| \leq \frac{3ML_H}{2} \|\mathbf{x}^k - \mathbf{x}^*\|^2 + \mathcal{O}(\|\epsilon^k\|), \quad \forall k \geq \hat{k},$$

where  $\nabla_{\mathcal{I}^* \mathcal{I}^*}^2 F(\mathbf{x})$  is locally Lipschitz continuous with constant  $L_H > 0$  on  $\mathcal{B}(\mathbf{x}^*, \rho)$ .

*Proof.* We can remove the subscript  $\mathcal{W}_k$  for simplicity by noting that the discussion is restricted within  $\mathcal{M}(\mathbf{x}^*, \boldsymbol{\epsilon}^*)$ . Given  $\nabla^2 F(\mathbf{x}^*)$  is nonsingular, we can select a sufficiently small  $\rho$  so that  $\nabla^2 F(\mathbf{x}^k; \boldsymbol{\epsilon}^k)$  is also nonsingular for any  $\|\mathbf{x}^k - \mathbf{x}^*\| < \rho$  and  $\|\boldsymbol{\epsilon}^k\| < \rho$ , since  $\nabla^2 F(\cdot; \boldsymbol{\epsilon})$  is continuous with respect to  $\boldsymbol{\epsilon}$ . We have from Corollary 1 that

$$\begin{aligned}\mathbf{x}^{k+1} - \mathbf{x}^* &= \mathbf{x}^k - \mathbf{x}^* - \nabla^2 F(\mathbf{x}^k; \boldsymbol{\epsilon}^k)^{-1} \nabla F(\mathbf{x}^k; \boldsymbol{\epsilon}^k) \\ &= \mathbf{x}^k - \mathbf{x}^* - \nabla^2 F(\mathbf{x}^k; \boldsymbol{\epsilon}^k)^{-1} (\nabla F(\mathbf{x}^k; \boldsymbol{\epsilon}^k) - \nabla F(\mathbf{x}^*)) \\ &= \nabla^2 F(\mathbf{x}^k; \boldsymbol{\epsilon}^k)^{-1} (\nabla F(\mathbf{x}^*) - \nabla F(\mathbf{x}^k; \boldsymbol{\epsilon}^k) - \nabla^2 F(\mathbf{x}^k; \boldsymbol{\epsilon}^k) (\mathbf{x}^* - \mathbf{x}^k)).\end{aligned}$$

It follows that

$$\begin{aligned}\|\mathbf{x}^{k+1} - \mathbf{x}^*\| &\leq \|\nabla^2 F(\mathbf{x}^k; \boldsymbol{\epsilon}^k)^{-1}\| \|\nabla F(\mathbf{x}^*) - \nabla F(\mathbf{x}^k; \boldsymbol{\epsilon}^k) - \nabla^2 F(\mathbf{x}^k; \boldsymbol{\epsilon}^k) (\mathbf{x}^* - \mathbf{x}^k)\| \\ &= \|\nabla^2 F(\mathbf{x}^k; \boldsymbol{\epsilon}^k)^{-1}\| \|\nabla F(\mathbf{x}^*) - \nabla F(\mathbf{x}^k) - \nabla^2 F(\mathbf{x}^k) (\mathbf{x}^* - \mathbf{x}^k) \\ &\quad + \nabla F(\mathbf{x}^k) - \nabla F(\mathbf{x}^k; \boldsymbol{\epsilon}^k) + [\nabla^2 F(\mathbf{x}^k) - \nabla^2 F(\mathbf{x}^k; \boldsymbol{\epsilon}^k)] (\mathbf{x}^* - \mathbf{x}^k)\|.\end{aligned}\tag{47}$$

Consider any  $\rho > 0$  and  $\mathbf{x}^k$  such that  $\|\mathbf{x}^k - \mathbf{x}^*\| \leq \rho < \frac{1}{2ML_H}$ . We have that

$$\begin{aligned}\|\nabla^2 F(\mathbf{x}^*)^{-1} (\nabla^2 F(\mathbf{x}^k) - \nabla^2 F(\mathbf{x}^*))\| &\leq \|\nabla^2 F(\mathbf{x}^*)^{-1}\| \|\nabla^2 F(\mathbf{x}^k) - \nabla^2 F(\mathbf{x}^*)\| \\ &\leq ML_H \|\mathbf{x}^k - \mathbf{x}^*\| \leq \rho ML_H \leq \frac{1}{2}.\end{aligned}$$

and

$$\|\nabla^2 F(\mathbf{x}^k)^{-1}\| \leq \frac{\|\nabla^2 F(\mathbf{x}^*)^{-1}\|}{1 - \|\nabla^2 F(\mathbf{x}^*)^{-1} (\nabla^2 F(\mathbf{x}^k) - \nabla^2 F(\mathbf{x}^*))\|} \leq 2M.\text{<sup>1</sup>}$$

We can then choose  $\rho$  even smaller such that

$$\|\nabla^2 F(\mathbf{x}^k; \boldsymbol{\epsilon}^k)^{-1}\| < 3M\tag{48}$$

for any  $\|\mathbf{x}^k - \mathbf{x}^*\| < \rho$  and  $\|\boldsymbol{\epsilon}^k\| < \rho$ .

On the other hand, there exists  $\hat{x}_i^k$  satisfying  $|\hat{x}_i^k| \in (|x_i^k|, |x_i^k| + \epsilon_i^k)$  and

$$|\lambda p(|x_i^k|)^{p-1} - \lambda p(|x_i^k| + \epsilon_i^k)^{p-1}| = \lambda p(p-1) |\hat{x}_i^k|^{p-2} \epsilon_i^k \leq \lambda p(p-1) \delta^{p-2} \epsilon_i^k,$$

where  $\delta > 0$  as defined in Proposition 6. Therefore, it holds that

$$\|\nabla F(\mathbf{x}^k) - \nabla F(\mathbf{x}^k; \boldsymbol{\epsilon}^k)\| \leq \lambda p(1-p) \delta^{p-2} \|\boldsymbol{\epsilon}^k\|.\tag{49}$$

In addition, there exists  $\hat{x}_i^k$  satisfying  $|\hat{x}_i^k| \in (|x_i^k|, |x_i^k| + \epsilon_i^k)$  and

$$\begin{aligned}|\lambda p(p-1)(|x_i^k|)^{p-2} - (|x_i^k| + \epsilon_i^k)^{p-2}| &= \lambda p(p-1)(p-2) |\hat{x}_i^k|^{p-3} \epsilon_i^k \\ &\leq \lambda p(p-1)(p-2) \delta^{p-3} \epsilon_i^k.\end{aligned}$$

---

<sup>1</sup>For matrices  $\mathbf{A}$  and  $\mathbf{B}$ , if  $\mathbf{A}$  is nonsingular and  $\|\mathbf{A}^{-1}(\mathbf{B} - \mathbf{A})\|_2 < 1$ , then  $\mathbf{B}$  is nonsingular and  $\|\mathbf{B}^{-1}\|_2 \leq \frac{\|\mathbf{A}^{-1}\|_2}{1 - \|\mathbf{A}^{-1}(\mathbf{B} - \mathbf{A})\|_2}$ .

Therefore, it holds that  $\|\nabla^2 F(\mathbf{x}^k) - \nabla^2 F(\mathbf{x}^k; \boldsymbol{\epsilon}^k)\| \leq \lambda p(p-1)(p-2)\delta^{p-3}\|\boldsymbol{\epsilon}^k\|$ , implying

$$\begin{aligned} & \|[\nabla^2 F(\mathbf{x}^k) - \nabla^2 F(\mathbf{x}^k; \boldsymbol{\epsilon}^k)](\mathbf{x}^* - \mathbf{x}^k)\| \\ & \leq \|\nabla^2 F(\mathbf{x}^k) - \nabla^2 F(\mathbf{x}^k; \boldsymbol{\epsilon}^k)\| \|\mathbf{x}^* - \mathbf{x}^k\| \leq \lambda p(p-1)(p-2)\delta^{p-3}\|\boldsymbol{\epsilon}^k\| \|\mathbf{x}^* - \mathbf{x}^k\|. \end{aligned} \quad (50)$$

Since  $\nabla F(\mathbf{x})$  is continuously differentiable on  $\mathcal{B}(\mathbf{x}^*, \rho)$  by Assumption 11, we know

$$\|\nabla F(\mathbf{x}^*) - \nabla F(\mathbf{x}^k) - \nabla^2 F(\mathbf{x}^k)(\mathbf{x}^* - \mathbf{x}^k)\| = \frac{L_H}{2} \|\mathbf{x}^k - \mathbf{x}^*\|^2. \quad (51)$$

Combining (47) with (48), (49), (50) and (51), we have for all  $\|\mathbf{x}^k - \mathbf{x}^*\| < \rho$  and  $\|\boldsymbol{\epsilon}^k\| < \rho$  that

$$\begin{aligned} \|\mathbf{x}^{k+1} - \mathbf{x}^*\| & \leq 3M\left(\frac{L_H}{2}\|\mathbf{x}^k - \mathbf{x}^*\|^2 + \lambda p(1-p)\delta^{p-2}\|\boldsymbol{\epsilon}^k\|\right. \\ & \quad \left. + \lambda p(p-1)(p-2)\delta^{p-3}\|\boldsymbol{\epsilon}^k\| \|\mathbf{x}^* - \mathbf{x}^k\|\right) \\ & \leq \frac{3ML_H}{2} \|\mathbf{x}^k - \mathbf{x}^*\|^2 + \mathcal{O}(\|\boldsymbol{\epsilon}^k\|). \end{aligned}$$

This completes the proof.  $\square$

## 4 Variants and Extensions

In this section, we discuss possible variants of solution methods to solve the QP subproblems, as well as the extension of SOIR $\ell_1$  to accommodate general nonconvex regularizers.

### 4.1 Variants of the QP subproblem

The QP subproblem solved in Lines 16–20 of Algorithm 1 seeks an inexact Newton direction restricted to a reduced space using subspace regularized Newton method. Proposition 6 and Theorem 7 indicate that the QP subproblem will be always triggered after some iteration. Therefore, we can consider replacing the Lines 16–20 of Algorithm 1 with a tailored trust-region subproblem, which reads

$$\mathbf{d}_{\mathcal{W}_k}^k = \arg \min_{\mathbf{d} \in \mathbb{R}^{|\mathcal{W}_k|}} \langle \mathbf{g}^k, \mathbf{d} \rangle + \frac{1}{2} \langle \mathbf{d}, \mathbf{H}^k \mathbf{d} \rangle + \frac{1}{2} \tau_H \|\mathbf{d}\|^2 \quad \text{s.t. } \|\mathbf{d}\| \leq \Delta_k \quad (52)$$

where  $\tau_H \in (0, \infty)$  and  $\Delta_k > 0$  refers to the trust region. The major difference between the trust region Newton subproblem and (29) includes: (i) The trust region Newton subproblem can accept non-convex  $\mathbf{H}^k$ . Although this requires a nonconvex QP subproblem solver, efficient subproblem solvers are presented in [46]. (ii) If the QP (52) yields a direction out of the current orthant, we project it back to the the current orthant. If such direction yields a non-increasing direction, then it is accepted; otherwise, the radius of the trust region is reduced. (iii) If the QP yields a direction to stay in the current orthant, then a classic trust-region update is executed.

In the trust region Newton subproblem, it can be easily shown that the descent amount of objective is bounded by the  $\|\mathbf{g}^k\|$ , therefore the global convergence result Theorem 8 can be obtained similarly, which are skipped here.

The algorithm locally always end in a trust region and direction within the current orthant, thus the smoothness assumption over  $\{\mathbf{x}^k, \mathbf{x}^k + \mathbf{d}^k\}$  is always satisfied [46, Assumption 1]. Therefore the algorithm locally reverts to the one presented in [46, Algorithm 1] and a similar convergence rate and convergence to a second-order optimal solution can be derived. The local convergence result is stated below.

**Theorem 13.** *Suppose the termination condition is set to*

$$\|\nabla F(\mathbf{x}^k, \epsilon^k)\| \leq \tau \text{ and } \lambda_{\min}(\nabla^2 F(\mathbf{x}^k, \epsilon^k)) \geq -\tau^{1/2},$$

*Assume that  $\mathcal{I}(\mathbf{x}^k) = \mathcal{I}^*$  for all  $k > \hat{k} > 0$ , then the trust region Newton subproblem is triggered successively, and the rest number of iterations  $\mathcal{K} := \{k \mid k > \hat{k}\}$  before termination satisfies*

$$|\mathcal{K}| = \tilde{\mathcal{O}}(\tau^{-3/2}).$$

Due to space limitations, we will not delve into the proof of the theorem which can be found in [46, Theorem]. The key point here is that the proposed algorithmic framework can potentially incorporate many variants of QP subproblems and locally revert to classic second-order methods.

## 4.2 Extension to general nonconvex regularization

We now extend SOIR $\ell_1$  to solve (1), as instanced by other nonconvex regularizers, see Table 2. First, the locally approximate model can be formulated as follows.

$$\min_{\mathbf{x} \in \mathbb{R}^n} \tilde{G}_k(\mathbf{x}) := f(\mathbf{x}) + \sum_{i=1}^n \omega_i^k |x_i|,$$

with  $\omega_i^k = r'(|x_i^k| + \epsilon_i^k)$ . Note that of  $r'(0^+) < +\infty$ , we can set  $\epsilon_i^k \equiv 0, \forall i \in [n]$ .

**Remark 5.** *We always require the condition  $|\nabla_i f(\mathbf{x})| < r'(0^+)$ . holds on the level set  $\text{Lev}_F$  described in Lemma 4. This condition appears in many nonsmooth optimization algorithms and generally takes the form  $0 \in \text{rnt}\partial F(\mathbf{x})$  for minimizing  $F$ . In our case, this condition can be satisfied by setting  $q$  in the regularizers in Table 2 sufficiently small.*

Throughout the analysis related to IST (i.e. Lemma 2, Proposition 6), it takes the forms of weighted  $\ell_1$  instead of  $\ell_p$ , therefore, we can achieve the same convergence results following the same analysis using Remark 5 and Assumption 1(ii).

## 5 Numerical Experiments

In this section, we deliver a set of numerical experiments using synthetic and real-world data to demonstrate the effectiveness of the proposed SOIR $\ell_1$  for solving the nonconvex  $\ell_p$ -regularized logistic regression problem [9, 49]. Specifically, by applying

**Table 2:** Examples of regularized functions and weight expressions

Regularizer	$r( \mathbf{x} )$	$[\omega(\mathbf{x})]_i = r'( \mathbf{x}_i )$	$r''( \mathbf{x}_i )$
LPN [2]	$\sum_{i=1}^n ( x_i )^q$	$q( x_i )^{q-1}$	$q(q-1)( x_i )^{q-2}$
LOG [47]	$\sum_{i=1}^n \log(1 + \frac{ x_i }{q})$	$\frac{1}{ x_i +q}$	$-\frac{1}{( x_i +q)^2}$
FRA [2]	$\sum_{i=1}^n \frac{ x_i }{ x_i +q}$	$\frac{q}{( x_i +q)^2}$	$-\frac{( x_i +q)^3}{2q x_i }$
TAN [10]	$\sum_{i=1}^n \arctan(\frac{ x_i }{q})$	$\frac{q}{q^2+( x_i )^2}$	$\frac{-2q x_i }{(q^2+ x_i ^2)^2}$
EXP [48]	$\sum_{i=1}^n 1 - e^{-\frac{ x_i }{q}}$	$\frac{1}{q} e^{-\frac{ x_i }{q}}$	$-\frac{1}{q^2} e^{-\frac{ x_i }{q}}$

$f(\mathbf{x}) = \sum_{i=1}^m \log(1 + e^{-a_i \mathbf{x}^T \mathbf{b}_i})$ , we consider solving

$$\min_{\mathbf{x} \in \mathbb{R}^n} \quad \sum_{i=1}^m \log(1 + e^{-a_i \mathbf{x}^T \mathbf{b}_i}) + \lambda \|\mathbf{x}\|_p^p, \quad (53)$$

where  $\lambda > 0$ , and  $a_i \in \{-1, 1\}$  and  $\mathbf{b}_i \in \mathbb{R}^n$ ,  $i \in [m]$  are the labels and feature vectors, respectively. In these numerical studies, we compare the proposed SOIR $\ell_1$  with several state-of-the-art algorithms to solve (53), including HpgSRN [33]<sup>2</sup>, PCSNP[34]<sup>3</sup> and EPIR $\ell_1$  [15]. All codes were implemented in MATLAB and executed on a PC equipped with an Intel i9-13900K 3.00 GHz CPU and 64 GB of RAM.

### 5.1 Experimental setup

The synthetic dataset is generated according to the methods presented in [36, 50]. Specifically, labels  $a_i, i \in [m]$  are drawn from a Bernoulli distribution and all feature vectors  $\mathbf{b}_i, i \in [m]$  are sampled from a standard Gaussian distribution. The real-world datasets *w8a*, *a9a*, *real-sim*, *gisette*, *news20*, and *rcv1.train* are binary classification examples downloaded from the LIBSVM repository<sup>4</sup>.

For SOIR $\ell_1$ , we set  $\lambda = 1, \gamma = 1, \eta_\Phi = 1, \eta_\Psi = 1, \tau = 10^{-8}, \alpha = 10^{-8}, \xi = 0.5$  and  $\varpi = 0.1$ . For the subspace quadratic subproblem in Lines 16-18, we adopt the truncated conjugate gradient method described in [36, Section 4.2] and we set  $\zeta_k = 10^{-8} + 10^{-4} \|\mathbf{g}^k\|^{0.5} + \delta^k$  with  $\delta^k = \min\{\lambda p(p-1) |x_i^k|^{p-2}, i \in \mathcal{I}(\mathbf{x}^k)\}$  to ensure  $\mathbf{H}^k \succ \mathbf{0}$ . For the tailored trust-region Newton subproblem presented in Section 4.1, we adopt the solver presented in [46, Algorithm 2]. In Lines 11 and 14, the initial stepsize  $\bar{\mu}$  is set by the classic Barzilai-Borwein (BB) rule [51]. We set  $\epsilon^0 = 1$  and update the perturbation  $\epsilon$  presented in Line 25 as follows

$$\epsilon_i^{k+1} = \begin{cases} 0.9\epsilon_i^k, & k \in \mathcal{S}_\Psi, i \in \mathcal{I}^{k+1}, \\ 0.9(\epsilon_i^k)^{1.1}, & k \in \mathcal{S}_\Phi, i \in \mathcal{I}^{k+1}, \\ \min\{0.9\epsilon_i^k, (\epsilon_i^k)^2\}, & k \in \mathcal{S}_{QP}, i \in \mathcal{I}^{k+1}, \\ \epsilon_i^k, & \text{otherwise.} \end{cases}$$

<sup>2</sup>The source code is available at <https://github.com/YuqiaWU/HpgSRN>

<sup>3</sup>The source code is available at <https://github.com/ShenglongZhou/PSNP>

<sup>4</sup>Refer to <https://www.csie.ntu.edu.tw/~cjlin/libsvmtools/datasets/>

Furthermore, before the iteration  $k$  enters  $\mathcal{S}_{QP}$ , we set  $\epsilon_i^k = \max\{\epsilon_i^k, 10^{-8}\}$  whenever  $k \in \mathcal{S}_\Psi \cup \mathcal{S}_\Phi$ . This adjustment ensures that perturbation values do not become excessively small.

The parameters for HpgSRN, PCSNP, and EPIR $\ell_1$  were chosen according to the suggestions provided in their respective papers. In particular, PCSNP addresses an  $\ell_2$ -norm regularized logistic regression problem. For the purpose of comparison, we set the  $\ell_2$ -norm regularization parameter  $\mu$  to 0, as specified in their study. For all algorithms, the initial point was set to  $\mathbf{x}^0 = \mathbf{0}$ .

## 5.2 Numerical Results

### 5.2.1 Local quadratic convergence behavior

We first demonstrate that SOIR $\ell_1$  exhibits a local quadratic convergence using both the synthetic dataset and six real-world dataset. Inspired by [52], our demonstration is based on the following two metrics:

$$\mathcal{R}_{\text{opt}}(\mathbf{x}) = \|\mathbf{x} \nabla f(\mathbf{x}) + \lambda p |\mathbf{x}|^p\|_\infty, \quad \text{and} \quad \mathcal{R}_{\text{dist}}(\mathbf{x}) = \|\mathbf{x} - \mathbf{x}^*\|_\infty,$$

where  $\mathbf{x}^*$  is the solution returned by SOIR $\ell_1$  and  $p = 0.5$ . Figure 1 displays  $\log_{10}(\mathcal{R}_{\text{opt}})$  and  $\log_{10}(\mathcal{R}_{\text{dist}})$  over the last ten iterations of Algorithm 1 for six real-world datasets (see panels (a) and (b)) and synthetic datasets with different sizes (see panels (c) and (d)). In particular, for the synthetic datasets, each was tested in 20 random trials, and the average results are highlighted. As shown in Figure 1, the slope in each subfigure is generally less than  $-2$ .

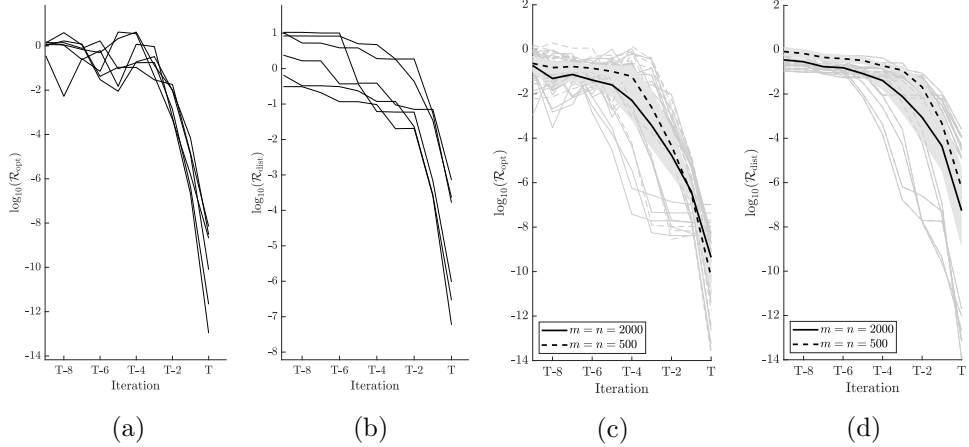


**Fig. 1:** Illustration of the local quadratic convergence behavior of SOIR $\ell_1$ .

### 5.2.2 Real-world datasets

In this subsection, we drive the performance comparison between SOIR $\ell_1$  with HpgSRN, PCSNP and EPIR $\ell_1$  on real-world datasets. Note that SOIR $\ell_1$ -RQP refers to SOIR $\ell_1$  that solves a regularized quadratic subproblem (29), while SOIR $\ell_1$ -TR refers to SOIR $\ell_1$  that solves a trust-region subproblem (52). For the second-order methods HpgSRN, PCSNP and SOIR $\ell_1$ , despite their original termination condition, in addition to the original termination criteria specified for each method, we also employed the condition  $\|\mathbf{x}^k - \mathbf{x}^{k-1}\|/\|\mathbf{x}^k\| < 10^{-9}$  to determine when to terminate the algorithm. For the first-order method EPIR $\ell_1$ , we maintain its original termination condition of  $\|\mathbf{x}^k - \mathbf{x}^{k-1}\|/\|\mathbf{x}^k\| < 10^{-4}$ .

To evaluate the performance of various methods, we consider the CPU time, objective value, and the sparsity level of the obtained solution (e.g., the percentage of zeros). Each presented results are averaged over 10 independent runs. In this test, we set  $p = 0.5$ .

The comparison results are presented in Table 3. From Table 3, it is evident that SOIR $\ell_1$ -RQP and SOIR $\ell_1$ -TR are generally efficient in terms of the running time while keeping achieving the lowest or near-lowest objective values. They also maintain a sparsity level comparable to other benchmark algorithms. During our numerical experiments, we observed that the Newton steps in PCSNP are infrequently triggered, which may account for the longer CPU time reflected in the results.

### 5.3 Extension to other nonconvex regularizers

In this subsection, we demonstrate the numerical results of applying SOIR $\ell_1$  for solving (53) with other nonconvex regularizers.

#### 5.3.1 More stringent $p$ values

In this test, we only view HpgSRN as the benchmark algorithm given the numerical performance comparisons presented in Table 3, and we further compare the numerical performance between SOIR $\ell_1$ -RQP and HpgSRN for solving (53) with more stringent  $p$  values. Specifically, we set  $p = 0.3$ .

Table 4 summarizes the comparisons in terms of CPU time and objective value. It is evident from the table that SOIR $\ell_1$ -RQP significantly outperforms HpgSRN, especially on large datasets such as *real-sim* and *news20*. For these datasets, HpgSRN's CPU time increases dramatically compared to the results shown in Table 3, while our method maintains scalable CPU time. Additionally, Figure 2 illustrates this difference with synthetic datasets, where our method demonstrates only relatively small increases in CPU time as the feature size grows, in contrast to the substantial increases observed with HpgSRN.

#### 5.3.2 Other nonconvex regularizers

To evaluate SOIR $\ell_1$  on various nonconvex regularization problems, we apply different nonconvex regularizers, as detailed in Table 2, to logistic regression using the *a9a*, *gisette*, and *rcv1.train* datasets. For these evaluations, we set  $q = 10^{-5}$  for the LOG regularizer and  $q = 0.1$  for the others. Figure 3 displays the logarithmic residuals over

**Table 3:** Performance comparison on real-world datasets with  $p = 0.5$ . The size of the feature matrix is enclosed in parentheses.

dataset	Algorithm	Time (s)	Objective	% of zeros
a9a (32561×123)	SOIR $\ell_1$ -RQP	<b>0.50</b>	<b>10579.4</b>	45.53%
	SOIR $\ell_1$ -TR	<b>0.42</b>	10588.5	46.34%
	HpgSRN	2.90	10583.3	53.01%
	PCSNP	4.45	10599.8	53.66%
	EPIRL1	5.99	<b>10570.5</b>	39.02%
w8a (49749×300)	SOIR $\ell_1$ -RQP	<b>0.61</b>	5873.8	37.00%
	SOIR $\ell_1$ -TR	<b>1.38</b>	5876.9	37.00%
	HpgSRN	2.01	<b>5856.5</b>	37.00%
	PCSNP	26.45	5870.9	37.67%
	EPIRL1	13.05	<b>5865.1</b>	38.00%
gisette (6000×5000)	SOIR $\ell_1$ -RQP	<b>35.07</b>	<b>176.4</b>	97.06%
	SOIR $\ell_1$ -TR	<b>32.71</b>	<b>176.2</b>	97.06%
	HpgSRN	36.58	177.0	96.92%
	PCSNP	288.32	182.3	97.14%
	EPIRL1	326.48	178.3	97.02%
real sim (72309×20958)	SOIR $\ell_1$ -RQP	<b>3.81</b>	<b>7121.6</b>	93.63%
	SOIR $\ell_1$ -TR	10.01	<b>7123.3</b>	93.63%
	HpgSRN	<b>6.80</b>	7262.3	94.47%
	PCSNP	38.73	7445.8	95.02%
	EPIRL1	33.48	7152.7	93.78%
rcv1.train (20242×47236)	SOIR $\ell_1$ -RQP	<b>1.59</b>	<b>2554.6</b>	99.10%
	SOIR $\ell_1$ -TR	3.95	<b>2558.9</b>	99.08%
	HpgSRN	<b>1.69</b>	2578.4	99.21%
	PCSNP	6.86	2652.9	99.26%
	EPIRL1	14.10	2562.9	99.13%
news20 (19996×1355191)	SOIR $\ell_1$ -RQP	<b>20.08</b>	4034.5	99.97%
	SOIR $\ell_1$ -TR	93.54	<b>3989.7</b>	99.97%
	HpgSRN	<b>23.74</b>	4171.3	99.97%
	PCSNP	179.61	4682.0	99.98%
	EPIRL1	207.05	<b>3983.6</b>	99.97%

**Table 4:** Comparison against HpgSRN with  $p = 0.3$  on real-world datasets.

	Dataset	news20	w8a	a9a	real sim	rcv1.train	gisette
SOIR $\ell_1$ -RQP	Time (s)	60.21	0.80	0.47	9.01	3.86	31.79
	Objective	3019.06	5825.87	10596.93	5669.32	1933.62	165.18
HpgSRN	Time (s)	1871.86	3.29	3.49	50.67	15.73	34.07
	Objective	3696.13	5802.88	10595.47	6099.26	2078.87	186.27

the last 10 iterations, where the residual is defined as  $\mathcal{R}_{\text{opt}} = \|\mathbf{x} \circ (\nabla f(\mathbf{x}) + \boldsymbol{\omega}(\mathbf{x}, \mathbf{0}) \circ \text{sgn}(\mathbf{x}))\|_\infty$ .

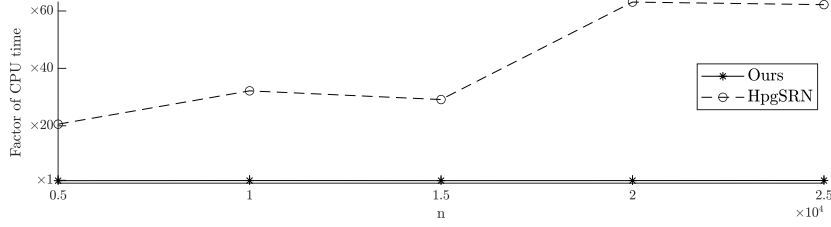


**Fig. 2:** Comparison against HpgSRN with  $p = 0.3$  on synthetic datasets.

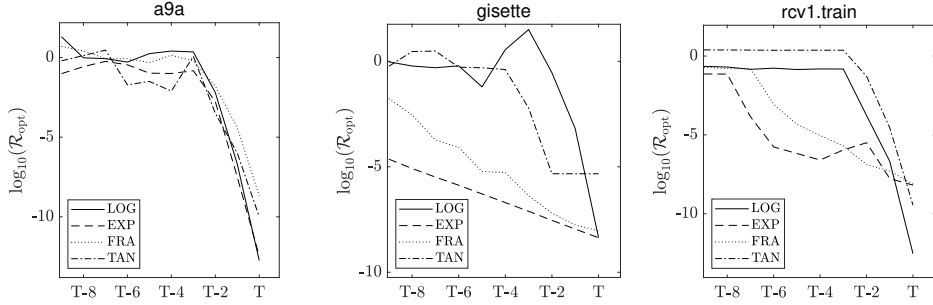


**Fig. 3:** Convergence results for other nonconvex regularizers on real-world datasets.

## 6 Conclusion

In this paper, we introduce a second-order iteratively reweighted  $\ell_1$  method for a class of nonconvex sparsity-promoting regularization problems. Our approach, by reformulating nonconvex regularization into weighted  $\ell_1$  form and incorporating subspace approximate Newton steps with subspace soft-thresholding steps, not only speeds up computation but also ensures algorithmic stability and convergence.

We prove global convergence under Lipschitz continuity and bounded Hessian conditions, achieving local superlinear convergence under KL property framework and local quadratic convergence with a strategic perturbation update. The method also extends to nonconvex and nonsmooth sparsity-driven regularization problems, maintaining similar convergence results. Empirical tests across various model prediction scenarios have demonstrated the method's effectiveness, suggesting its utility for complex optimization challenges in sparsity and nonconvexity contexts.

## Acknowledgments

We would like to acknowledge the support for this paper from the Young Scientists Fund of the National Natural Science Foundation of China No. 12301398.

## Appendix

**Lemma A.** Let  $d(\mu) = \mathcal{S}_{\mu\omega}(\mathbf{x} - \mu\mathbf{g}) - \mathbf{x}$  for  $\mu > 0$  where  $\mathbf{x}, \mathbf{g} \in \mathbb{R}^n$  and  $\omega \in \mathbb{R}_{++}^n$ . It holds that

$$d_i(\mu) = \mu d_i(1) \quad \text{if } x_i = 0, \quad (1a)$$

$$|d_i(\mu)| \geq \min\{\mu, 1\}|d_i(1)| \quad \text{if } x_i \neq 0. \quad (1b)$$

Moreover, for  $\omega_i > |g_i - x_i/\mu|$ ,  $d_i(\mu) = -x_i$ .

*Proof.* It holds from the soft-thresholding operator that

$$d_i(\mu) = \begin{cases} -\mu(g_i + \omega_i), & \text{if } \mu(g_i + \omega_i) < x_i, \\ -\mu(g_i - \omega_i), & \text{if } \mu(g_i - \omega_i) > x_i, \\ -x_i, & \text{otherwise.} \end{cases}$$

If  $i \in \mathcal{I}_0(\mathbf{x})$ ,  $x_i = 0$ . It is obvious that (1a) holds. If  $i \in \mathcal{I}(\mathbf{x})$ ,  $x_i \neq 0$ . We check the values of  $d_i(1)$ . If  $d_i(1) = -(g_i + \omega_i)$ , which means

$$g_i + \omega_i < x_i \quad (2)$$

by the expression of  $d_i(1)$ , we consider the order of  $x_i, \mu(g_i + \omega_i), \mu(g_i - \omega_i)$ .

Case (a):  $\mu(g_i - \omega_i) < \mu(g_i + \omega_i) < x_i$ , this belongs to the first case in  $d_i(\mu)$ , meaning  $d_i(\mu) = -\mu d_i(1)$ .

Case (b):  $\mu(g_i - \omega_i) \leq x_i \leq \mu(g_i + \omega_i)$ , this belongs to the third case in  $d_i(\mu)$ , so that  $d_i(\mu) = -x_i$ . It follows from (2) that

$$g_i + \omega_i < x_i < \mu(g_i + \omega_i),$$

meaning  $0 < g_i + \omega_i < x_i, \mu > x_i/(g_i + \omega_i) > 1$  or  $g_i + \omega_i < x_i < 0, \mu < x_i/(g_i + \omega_i) < 1$  by noticing (2). In either case,  $|x_i| > \min(\mu, 1)|g_i + \omega_i|$ , meaning  $|d_i(\mu)| > \min(\mu, 1)|d_i(1)|$ .

Case (c):  $x_i < \mu(g_i - \omega_i) < \mu(g_i + \omega_i)$ , this belongs to the second case in  $d_i(\mu)$ , so that  $d_i(\mu) = -\mu(g_i - \omega_i)$ . It follows from (2) that

$$g_i + \omega_i < \mu(g_i - \omega_i) < \mu(g_i + \omega_i), \quad (3)$$

meaning  $\nabla_i f(\mathbf{x}) + \omega_i > 0, \mu > 1$  or  $\nabla_i f(\mathbf{x}) + \omega_i < 0, \mu < 1$ . In either case, (3) implies that  $|\mu(g_i - \omega_i)| > \min(\mu, 1)|g_i + \omega_i|$ , indicating  $|d_i(\mu)| > \min(\mu, 1)|d_i(1)|$ .

If  $d_i(1) = -(g_i - \omega_i)$ , this means  $g_i + \omega_i < x_i$ . same argument based on the order of we consider the order of  $x_i, \mu(g_i + \omega_i), \mu(g_i - \omega_i)$  also yields (1b)

If  $d_i(1) = -x_i$ , this means  $g_i + \omega_i > x_i > g_i - \omega_i$ , the same argument based on the order of we consider the order of  $x_i, \mu(g_i + \omega_i), \mu(g_i - \omega_i)$  also yields (1b).  $\square$

## References

- [1] Rockafellar, R.T., Wets, R.J.-B.: *Variational Analysis* vol. 317. Springer, Heidelberg, Germany (2009)
- [2] Fazel, M., Hindi, H., Boyd, S.P.: Log-det heuristic for matrix rank minimization with applications to hankel and euclidean distance matrices. In: *Proceedings of the 2003 American Control Conference*, vol. 3, pp. 2156–2162 (2003). IEEE
- [3] Fan, J., Li, R.: Variable selection via nonconcave penalized likelihood and its oracle properties. *Journal of the American Statistical Association* **96**(456), 1348–1360 (2001)
- [4] Zhang, C.-H.: Nearly unbiased variable selection under minimax concave penalty. *The Annals of Statistics* **38**(2), 894–942 (2010)
- [5] Zhang, T.: Analysis of multi-stage convex relaxation for sparse regularization. *Journal of Machine Learning Research* **11**(3) (2010)
- [6] Chartrand, R.: Exact reconstruction of sparse signals via nonconvex minimization. *IEEE Signal Processing Letters* **14**(10), 707–710 (2007)
- [7] Gazzola, S., Nagy, J.G., Landman, M.S.: Iteratively reweighted FGMRES and FLSQR for sparse reconstruction. *SIAM Journal on Scientific Computing* **43**(5), 47–69 (2021)
- [8] Zhou, X., Liu, X., Wang, C., Zhai, D., Jiang, J., Ji, X.: Learning with noisy labels via sparse regularization. In: *Proceedings of the IEEE/CVF International Conference on Computer Vision*, pp. 72–81 (2021)
- [9] Liu, Z., Jiang, F., Tian, G., Wang, S., Sato, F., Meltzer, S.J., Tan, M.: Sparse logistic regression with  $\ell_p$  penalty for biomarker identification. *Statistical Applications in Genetics and Molecular Biology* **6**(1) (2007)
- [10] Candes, E.J., Wakin, M.B., Boyd, S.P.: Enhancing sparsity by reweighted  $\ell_1$  minimization. *Journal of Fourier Analysis and Applications* **14**, 877–905 (2008)
- [11] Hu, Y., Li, C., Meng, K., Qin, J., Yang, X.: Group sparse optimization via  $\ell_{p,q}$  regularization. *The Journal of Machine Learning Research* **18**(1), 960–1011 (2017)
- [12] Lu, Z.: Iterative reweighted minimization methods for  $\ell_p$  regularized unconstrained nonlinear programming. *Mathematical Programming* **147**(1-2), 277–307 (2014)
- [13] Wang, H., Zeng, H., Wang, J., Wu, Q.: Relating  $\ell_p$  regularization and reweighted  $\ell_1$  regularization. *Optimization Letters* **15**(8), 2639–2660 (2021)

- [14] Wang, H., Zeng, H., Wang, J.: Convergence rate analysis of proximal iteratively reweighted  $\ell_1$  methods for  $\ell_p$  regularization problems. *Optimization Letters* **17**(2), 413–435 (2023)
- [15] Wang, H., Zeng, H., Wang, J.: An extrapolated iteratively reweighted  $\ell_1$  method with complexity analysis. *Computational Optimization and Applications* **83**(3), 967–997 (2022)
- [16] Lai, M.-J., Xu, Y., Yin, W.: Improved iteratively reweighted least squares for unconstrained smoothed  $\ell_q$  minimization. *SIAM Journal on Numerical Analysis* **51**(2), 927–957 (2013)
- [17] Chen, X., Niu, L., Yuan, Y.: Optimality conditions and a smoothing trust region newton method for non-Lipschitz optimization. *SIAM Journal on Optimization* **23**(3), 1528–1552 (2013)
- [18] Chen, X., Zhou, W.: Convergence of the reweighted  $\ell_1$  minimization algorithm for  $\ell_2 - \ell_p$  minimization. *Computational Optimization and Applications* **59**(1-2), 47–61 (2014)
- [19] Chen, X., Zhou, W.: Convergence of reweighted  $\ell_1$  minimization algorithms and unique solution of truncated  $\ell_p$  minimization. Department of Applied Mathematics, The Hong Kong Polytechnic University (2010)
- [20] Xu, Z., Chang, X., Xu, F., Zhang, H.:  $l_{1/2}$  regularization: A thresholding representation theory and a fast solver. *IEEE Transactions on Neural Networks and Learning Systems* **23**(7), 1013–1027 (2012)
- [21] Lai, M.-J., Wang, J.: An unconstrained  $\ell_q$  minimization with  $0 < q \leq 1$  for sparse solution of underdetermined linear systems. *SIAM Journal on Optimization* **21**(1), 82–101 (2011)
- [22] Yu, P., Pong, T.K.: Iteratively reweighted  $\ell_1$  algorithms with extrapolation. *Computational Optimization and Applications* **73**(2), 353–386 (2019)
- [23] Liu, Y., Lin, R.: A bisection method for computing the proximal operator of the  $\ell_p$ -norm for any  $0 < p < 1$  with application to schatten p-norms. *Journal of Computational and Applied Mathematics* **447**, 115897 (2024)
- [24] Hu, Y., Li, C., Meng, K., Yang, X.: Linear convergence of inexact descent method and inexact proximal gradient algorithms for lower-order regularization problems. *Journal of Global Optimization* **79**(4), 853–883 (2021)
- [25] Mordukhovich, B.S., Yuan, X., Zeng, S., Zhang, J.: A globally convergent proximal newton-type method in nonsmooth convex optimization. *Mathematical Programming* **198**(1), 899–936 (2023)

- [26] Yue, M.-C., Zhou, Z., So, A.M.-C.: A family of inexact sqa methods for non-smooth convex minimization with provable convergence guarantees based on the Luo–Tseng error bound property. *Mathematical Programming* **174**(1), 327–358 (2019)
- [27] Liu, R., Pan, S., Wu, Y., Yang, X.: An inexact regularized proximal newton method for nonconvex and nonsmooth optimization. *Computational Optimization and Applications*, 1–39 (2024)
- [28] Burke, J.V., Moré, J.J.: On the identification of active constraints. *SIAM Journal on Numerical Analysis* **25**(5), 1197–1211 (1988)
- [29] Liang, J., Fadili, J., Peyré, G.: Activity identification and local linear convergence of forward–backward-type methods. *SIAM Journal on Optimization* **27**(1), 408–437 (2017)
- [30] Themelis, A., Stella, L., Patrinos, P.: Forward-backward envelope for the sum of two nonconvex functions: Further properties and nonmonotone linesearch algorithms. *SIAM Journal on Optimization* **28**(3), 2274–2303 (2018)
- [31] Themelis, A., Ahookhosh, M., Patrinos, P.: On the acceleration of forward-backward splitting via an inexact newton method. *Splitting Algorithms, Modern Operator Theory, and Applications*, 363–412 (2019)
- [32] Bareilles, G., Iutzeler, F., Malick, J.: Newton acceleration on manifolds identified by proximal gradient methods. *Mathematical Programming* **200**(1), 37–70 (2023)
- [33] Wu, Y., Pan, S., Yang, X.: A regularized Newton method for  $\ell_q$ -norm composite optimization problems. *SIAM Journal on Optimization* **33**(3), 1676–1706 (2023)
- [34] Zhou, S., Xiu, X., Wang, Y., Peng, D.: Revisiting  $\ell_q$  ( $0 \leq q < 1$ ) norm regularized optimization. *arXiv preprint arXiv:2306.14394* (2023)
- [35] Wang, H., Zhang, F., Shi, Y., Hu, Y.: Nonconvex and nonsmooth sparse optimization via adaptively iterative reweighted methods. *Journal of Global Optimization* **81**, 717–748 (2021)
- [36] Chen, T., Curtis, F.E., Robinson, D.P.: A reduced-space algorithm for minimizing  $\ell_1$ -regularized convex functions. *SIAM Journal on Optimization* **27**(3), 1583–1610 (2017)
- [37] Hager, W.W., Zhang, H.: A survey of nonlinear conjugate gradient methods. *Pacific Journal of Optimization* **2**(1), 35–58 (2006)
- [38] Bolte, J., Sabach, S., Teboulle, M.: Proximal alternating linearized minimization for nonconvex and nonsmooth problems. *Mathematical Programming* **146**(1), 459–494 (2014)

- [39] Li, G., Pong, T.K.: Calculus of the exponent of Kurdyka–Łojasiewicz inequality and its applications to linear convergence of first-order methods. *Foundations of Computational Mathematics* **18**(5), 1199–1232 (2018)
- [40] Luo, Z.-Q., Pang, J.-S., Ralph, D.: *Mathematical Programs with Equilibrium Constraints*. Cambridge University Press, Cambridge (1996)
- [41] Zeng, J., Lin, S., Xu, Z.: Sparse regularization: Convergence of iterative jumping thresholding algorithm. *IEEE Transactions on Signal Processing* **64**(19), 5106–5118 (2016)
- [42] Lewis, A.S.: Active sets, nonsmoothness, and sensitivity. *SIAM Journal on Optimization* **13**(3), 702–725 (2002) <https://doi.org/10.1137/S1052623401387623>
- [43] Attouch, H., Bolte, J., Svaiter, B.F.: Convergence of descent methods for semi-algebraic and tame problems: proximal algorithms, forward–backward splitting, and regularized Gauss–Seidel methods. *Mathematical Programming* **137**(1-2), 91–129 (2013)
- [44] Attouch, H., Bolte, J.: On the convergence of the proximal algorithm for non-smooth functions involving analytic features. *Mathematical Programming* **116**, 5–16 (2009)
- [45] Wen, B., Chen, X., Pong, T.K.: A proximal difference-of-convex algorithm with extrapolation. *Computational Optimization and Applications* **69**(2), 297–324 (2018)
- [46] Curtis, F.E., Robinson, D.P., Royer, C.W., Wright, S.J.: Trust-region Newton-CG with strong second-order complexity guarantees for nonconvex optimization. *SIAM Journal on Optimization* **31**(1), 518–544 (2021)
- [47] Lobo, M.S., Fazel, M., Boyd, S.: Portfolio optimization with linear and fixed transaction costs. *Annals of Operations Research* **152**, 341–365 (2007)
- [48] Bradley, P.S., Mangasarian, O.L., Street, W.N.: Feature selection via mathematical programming. *INFORMS Journal on Computing* **10**(2), 209–217 (1998)
- [49] Richard, M., Brian, D.: Design of maximally sparse beamforming arrays. *IEEE Trans. Antennas Propag* **39**(8), 1178–1187 (1991)
- [50] Keskar, N., Nocedal, J., Öztoprak, F., Waechter, A.: A second-order method for convex  $\ell_1$ -regularized optimization with active-set prediction. *Optimization Methods and Software* **31**(3), 605–621 (2016)
- [51] Barzilai, J., Borwein, J.M.: Two-point step size gradient methods. *IMA Journal of Numerical Analysis* **8**(1), 141–148 (1988)

[52] Burke, J.V., Curtis, F.E., Wang, H.: A sequential quadratic optimization algorithm with rapid infeasibility detection. *SIAM Journal on Optimization* **24**(2), 839–872 (2014)